Two-scale model for the effect of physical aging in elastomers filled with hard nanoparticles

Two-scale model for the effect of physical aging in elastomers filled with hard nanoparticles

Mykhailo Semkiv[a, b], E-mail: m.semkiv@tue.nl
Patrick D. Anderson[a], E-mail: p.d.anderson@tue.nl
Markus Hütter[a], E-mail: m.huetter@tue.nl

[a]Eindhoven University of Technology, Polymer Technology,
Department of Mechanical Engineering,
PO Box 513, 5600 MB Eindhoven, The Netherlands
[b]Dutch Polymer Institute (DPI),
P.O. Box 902, 5600 AX Eindhoven, The Netherlands

Abstract:

A two-scale model is developed, and solved numerically, to describe the mechanical behavior of elastomers filled with hard nanoparticles. Of particular interest is the slow recovery of the elastic modulus after large-amplitude oscillatory deformation. To account for this effect, the physical aging of the glassy bridges between the filler particles is captured with two thermal degrees of freedom for the matrix material, namely a kinetic and a configurational one. Formulating the two-scale model enriched with aging in a nonequilibrium thermodynamics context, first results in a constitutive relation for the Cauchy stress tensor. Second, the dynamics of physical aging is described, which eventually results in the slow recovery of the elastic modulus with waiting time. The proposed model is investigated numerically under large amplitude oscillatory shear deformation. Of particular interest in this respect is the coupling of the micro-scale dynamics with the physical aging on the macroscopic scale. This coupling is examined in detail, both in an approximate way using a Gaussian approximation, as well as numerically, under specific conditions. It turns out that the CONNFFESSIT approach (M. Laso, H. C. Öttinger, J. Non-Newtonian Fluid Mech., 47:1–20, 1993) can not be employed for the numerical solution of the model under arbitrary loading conditions because of the novel structure of the two-level coupling term. While a procedure for solving the model numerically for the case of strong applied deformation is presented in this paper, other solution methodologies need to be sought for the cases of weak and no applied deformation.

Keywords:

Silica-filled elastomers, two-scale model, physical aging, mechanical rejuvenation, nonequilibrium thermodynamics

1 Introduction

Composite materials, being widely used in different practical applications due to their remarkable properties, are of great interest to researchers concerned with fundamental modeling. This is because the behavior of entire system is the result of an intricate combination and coupling of dynamics on different length- as well as time-scales. The particular interest of this paper is the analytical modeling and numerical simulation of the mechanical behavior of composites that consist of an elastomer matrix filled with hard particles of nanometers size.

Filling an elastomer with nanoparticles adds significant rate-dependence to its mechanical behavior, and thus results in increased dissipation, as compared to the unfilled elastomer [1]. A possible expla-

nation, that is used in this paper as a basis for the model formulation, for these significant changes in the material behavior is the following. If the matrix material adheres well to the filler particle surface, the mobility in the matrix is slowed down close to these surfaces. More specifically, the mobility in a matrix material element is decreased gradually the closer this element is located to the filler particle surface. Effectively, this can be captured by an increase in the local glass transition temperature of matrix material as the distance to the filler particle surface decreases. If, in close enough vicinity to the particle surface, the local glass transition temperature is higher than the actual (laboratory) temperature, an effective glassy layer is present around the filler particle. At high enough volume fraction of filler particles and in a certain temperature regime, these glassy layers may then overlap, thereby creating so-called glassy bridges between the filler particles. Therefore, such composites consist essentially of a rubbery-state elastomer matrix that is permeated by a glassy network with filler particles, leading in mechanical reinforcements of up to about 100 times. The existence of glassy layers around filler particles is supported by the literature, e.g. by NMR studies [2] or more recently by a mechanical analysis of model systems [3, 4]. For more details on this issue, the reader is referred to, e.g., [5] and references therein.

Once the glassy bridges are formed between the particles, the interparticle dynamics can be analyzed in terms of the knowledge about the thermo-mechanics of bulk polymer glasses [6, 7]. Specific features of bulk polymer glasses that are relevant also for the glassy-bridge induced effects are the viscoplastic yielding behavior and strain softening, as well as the effect of physical aging on the mechanical behavior. For example, when making use of bulk yielding kinetics in the nanocomposite context, one can rationalize the highly nonlinear rate-dependent mechanical response of such nanocomposites, including the prominent Payne effect [5, 8–10].

In an earlier publication, a thermodynamically-inspired concurrent two-scale model has been developed to describe the mechanical behavior of elastomers filled with hard nanoparticles [5]. While that model takes the yielding kinetics of the glassy bridges into account, the physical aging of the glassy bridges is neglected. However, it is assumed that the physical aging of the glassy bridges may be related to the so-called Mullins effect in cyclic deformation [11–13]. This effect consists in a softening due to mechanical deformation, however, that softening is only present at strains smaller than the maximal previously applied strain. If the material is loaded beyond the maximal previously applied strain, initially no softening is present at these previously unvisited strains, while after repeated loading to these higher strains there is again softening. It has been found that the softening is not permanent, but that e.g. the permanent set or the complete stress-strain response can recover (partly) at a rate that is temperature-dependent, which is also sometimes called 'healing' [11–14]. Modeling the Mullins effect in terms of an extended two-scale model is beyond the scope of this paper. However, in order to embark towards this long-term goal, this paper aims at studying the effect of physical aging of the interparticle matrix material on the mechanical response of the entire composite. Specifically, the deformation protocol of [8, 9] is employed, that consists of a specific combination of mechanical rejuvenation (softening) and physical aging. Since the proper description of physical aging is rather involved and a topic of current research activities in the literature, the modeling effort for the case of nanocomposites can be split into two steps. First, the physical aging and mechanical rejuvenation can be studied from a thermodynamic perspective for bulk glassy polymers, e.g. as done in [15–18]. Second, the lessons learned from that latter work can be built into the two-scale nanocomposite model developed in [5], which is the topic of this paper.

The manuscript is organized as follows. In Sec. 2, the general equation for the nonequilibrium reversible-irreversible coupling (GENERIC) framework of nonequilibrium thermodynamics is introduced, followed by its application to the model developed for nanoparticle-filled elastomers in Sec. 3. The general concurrent two-scale model is summarized in Sec. 3.5. In Sec. 4, this model is made material-specific, whereafter it is analyzed numerically for illustration purposes by means of CONNFFESSIT-type simulations in Sec. 5. Finally, conclusions are drawn in Sec. 6.

Before we start, let us comment about the notation used throughout the entire paper. Greek indices α, β, γ, ... are used for the Cartesian components of vectors and tensors, and Einstein's summation convention is used for indices that occur twice. Furthermore, with respect to operators, subscripts α and (α, β) imply contraction with any vector A_α and any tensor $A_{\alpha\beta}$ multiplied from the left, respectively, while subscripts γ and (γ, ε) imply contraction with the vector A_γ and tensor $A_{\gamma\varepsilon}$ multiplied from the right, respectively. An analogous notation is used for continuous indices. Specifically, let $\boldsymbol{\xi}$ denote the position in the space of (micro-)states. If a generalized field depends on $\boldsymbol{\xi}$, this implies continuous contraction (i.e. integration) over $\boldsymbol{\xi}$ with what is multiplied from the left, while a dependence on $\boldsymbol{\xi}'$

implies continuous contraction (i.e. integration) over $\boldsymbol{\xi}'$ with what is multiplied from the right. Finally, it is mentioned that boundary terms are neglected entirely, because the main goal of this paper is the modeling of bulk material behavior. In contrast, the case where boundaries and interaction with the surrounding are of interest has been studied, e.g. in [19, 20].

2 GENERIC framework

The framework used in this paper to formulate the dynamics of the system is the general equation for the nonequilibrium reversible-irreversible coupling (GENERIC) [21–23], which has also been used in our preceding work [5, 17, 18]. It is a formal thermodynamic procedure to set up evolution equations for a set of variables $\boldsymbol{\mathcal{X}}$. In this section, we recapitulate the explanation of the methodology given in [17]. Specifically, in the GENERIC framework, the reversible ("rev") and irreversible ("irr") contributions are clearly distinguished,

$$\partial_t \boldsymbol{\mathcal{X}} = \partial_t \boldsymbol{\mathcal{X}}|_{\mathrm{rev}} + \partial_t \boldsymbol{\mathcal{X}}|_{\mathrm{irr}} \,, \tag{1}$$

with

$$\partial_t \boldsymbol{\mathcal{X}}|_{\mathrm{rev}} = \boldsymbol{\mathcal{L}} \frac{\delta E}{\delta \boldsymbol{\mathcal{X}}} \,, \tag{2}$$

$$\partial_t \boldsymbol{\mathcal{X}}|_{\mathrm{irr}} = \boldsymbol{\mathcal{M}} \frac{\delta S}{\delta \boldsymbol{\mathcal{X}}} \,, \tag{3}$$

where ∂_t denotes the partial derivative with respect to time t. The reversible dynamics is driven by the gradient of energy E, mediated by the Poisson operator $\boldsymbol{\mathcal{L}}$, while the irreversible dynamics is driven by the gradient of entropy S, mediated by the friction matrix $\boldsymbol{\mathcal{M}}$. As part of the GENERIC structure, on the one hand, the reversible dynamics must not change the entropy, and the Poisson operator must be skew-symmetric and satisfy the Jacobi-identity, i.e.,

$$\boldsymbol{\mathcal{L}} \frac{\delta S}{\delta \boldsymbol{\mathcal{X}}} = 0 \,, \tag{4}$$

$$\boldsymbol{\mathcal{L}}^{\mathrm{T}} = -\boldsymbol{\mathcal{L}} \,, \tag{5}$$

$$\{A, \{B, C\}\} + \{B, \{C, A\}\} + \{C, \{A, B\}\} = 0 \,, \tag{6}$$

with the Poisson bracket defined by $\{A, B\} = \langle \delta A/\delta \boldsymbol{\mathcal{X}}, \boldsymbol{\mathcal{L}}\, \delta B/\delta \boldsymbol{\mathcal{X}} \rangle$ based on the inner product $\langle \cdot, \cdot \rangle$, and functionals A, B, and C. With these conditions, the Hamiltonian structure of the reversible dynamics is guaranteed, and specifically the time-structure invariance is respected by way of the Jacobi identity [23]. On the other hand, the irreversible dynamics must not change the energy, and the friction matrix must be symmetric and be positive semi-definite, i.e.,

$$\boldsymbol{\mathcal{M}} \frac{\delta E}{\delta \boldsymbol{\mathcal{X}}} = 0 \,, \tag{7}$$

$$\boldsymbol{\mathcal{M}}^{\mathrm{T}} = \boldsymbol{\mathcal{M}} \,, \tag{8}$$

$$\boldsymbol{\mathcal{M}} \geq 0 \,. \tag{9}$$

The resulting irreversible dynamics is thus a generalization of the Ginzburg-Landau equation. The reversible (2) and irreversible (3) contributions are coupled by the degeneracy conditions (4) and (7). About (8) it must be said that the friction matrix $\boldsymbol{\mathcal{M}}$ in general is Onsager-Casimir symmetric, as will be discussed below. For more details on the Onsager-Casimir symmetry, the reader is also referred to [21–23].

3 Model development

3.1 Dynamic variables and generating functionals

The state of deformation of a purely elastic material can be quantified by the deformation gradient $\boldsymbol{F}$. This quantity contains also the mass density, $\rho = \rho_0 / \det \boldsymbol{F}$ with ρ_0 the mass density in the undeformed

state. To describe the evolution of the material deformation, the velocity field $\boldsymbol{v}$ or the momentum density $\boldsymbol{m} = \rho\boldsymbol{v}$ are suitable candidates. While all these quantities are macroscopic, the microstructure in terms of the arrangement of the filler particles in the elastomer matrix is of interest as well, as discussed in the Introduction, Sec. 1. It has been discussed in detail in [5] that, in order to strike a balance between detail and model efficiency, it is useful to consider a single representative filler-particle pair only, instead of a large number of filler particles. Particularly, if $\boldsymbol{R}$ denotes the actual particle separation vector of the representative particle pair, and $\boldsymbol{Q}$ is the particle separation vector in the corresponding mechanically unloaded state, then the distribution function $p(\boldsymbol{r}, \boldsymbol{R}, \boldsymbol{Q})$ is a useful microstructural quantity, which also depends on macroscopic position $\boldsymbol{r}$. The normalization of $p(\boldsymbol{r}, \boldsymbol{R}, \boldsymbol{Q})$ is such that integration over $\boldsymbol{R}$ and $\boldsymbol{Q}$ leads to the number density of (representative) particle pairs per unit volume [5].

In [5], this just discussed set of variables is augmented by the absolute temperature T in order to account for the thermal state and to be able to model nonisothermal processes. However, it turns out that for the extension sought in this paper, namely the extension of [5] to account for the physical aging of the glassy bridges, the model formulation simplifies drastically when using the total entropy density per unit volume s_t, including all entropy contributions of the elastomer matrix as well as of the filler-particle arrangement.

To describe the physical aging of the glassy bridges, one needs to be able to model the physical aging of the glassy matrix material. As discussed in detail in [17,18] and references therein, a practical way to achieve that is by accounting for an additional thermal variable. This is needed in order to mimic the fact that, in the glassy state, there is a substantial difference between the (rapid) relaxation and equilibration of vibrations around energy minima on the one hand, and on the other hand the population of different low-energy states by way of transitions across high energy barriers (by rare events). This discrepancy in dynamics can be captured by splitting the total entropy of the glassy material into its so-called kinetic (s) and configurational (η) parts, where the former describes the local intra-basin dynamics in the energy landscape, while the latter describes the much slower inter-basin dynamics [17,18]. For the current study, however, one notices that only η needs to be included in the set of variables, while s can be obtained by subtracting η and the filler particle entropy from s_t.

In summary, the complete set of independent dynamic variables in an Eulerian (i.e. spatial) setting for the model formulation in this paper is chosen as

$$\boldsymbol{\mathcal{X}} = \big(\boldsymbol{m}(\boldsymbol{r}),\, s_\mathrm{t}(\boldsymbol{r}),\, \eta(\boldsymbol{r}),\, \boldsymbol{F}(\boldsymbol{r}),\, p(\boldsymbol{r}, \boldsymbol{\xi})\big), \tag{10}$$

with macroscopic position $\boldsymbol{r}$, momentum density $\boldsymbol{m}$, total entropy density of elastomer matrix plus filler particles s_t, configurational entropy density of the elastomer matrix η, deformation gradient $\boldsymbol{F}$, and the filler particle arrangement described by p with $\boldsymbol{\xi} = (\boldsymbol{R}, \boldsymbol{Q})$. Note that also previously entropies have been used to model the effect of physical aging in glassy systems [16, 24, 25].

The total energy and the total entropy of the system in terms of the complete set of variables $\boldsymbol{\mathcal{X}}$ can be written in the form

$$E = \int \frac{m_\gamma m_\gamma}{2\rho}\, d^3\boldsymbol{r} + U\left[s_\mathrm{t}, \eta, \boldsymbol{F}, p\right], \tag{11}$$

$$S = \int s_\mathrm{t}\, d^3\boldsymbol{r}, \tag{12}$$

with U the non-kinetic, i.e. internal, energy contribution that is a yet unspecified functional of its arguments. The gradients of energy and entropy with respect to $\boldsymbol{\mathcal{X}}$ are then given by

$$\frac{\delta E}{\delta \boldsymbol{\mathcal{X}}} = \left(\boldsymbol{v},\, \frac{\delta U}{\delta s_\mathrm{t}}\bigg|_{\eta,\boldsymbol{F},p},\, \frac{\delta U}{\delta \eta}\bigg|_{s_\mathrm{t},\boldsymbol{F},p},\, \frac{\delta U}{\delta \boldsymbol{F}}\bigg|_{s_\mathrm{t},\eta,p} - \frac{\boldsymbol{v}^2}{2}\rho_{,\boldsymbol{F}}\,,\, \frac{\delta U}{\delta p}\bigg|_{s_\mathrm{t},\eta,\boldsymbol{F}}\right), \tag{13}$$

$$\frac{\delta S}{\delta \boldsymbol{\mathcal{X}}} = (\boldsymbol{0},\, 1,\, 0,\, \boldsymbol{0},\, 0)\,. \tag{14}$$

For the sake of simplifying the notation, the following abbreviations for the derivatives of the energy with respect to the entropies are introduced,

$$T_1 = \frac{\delta U}{\delta s_\mathrm{t}}\bigg|_{\eta,\boldsymbol{F},p}, \tag{15}$$

$$T_2 = \frac{\delta U}{\delta \eta}\bigg|_{s_\mathrm{t},\boldsymbol{F},p}. \tag{16}$$

At this point, the quantities T_1 and T_2 are no more than mere abbreviations for the functional derivatives. Their physical meaning will be explained in the following.

3.2 Physical meaning of the temperatures T_1 and T_2

In order to give a physical interpretation of the temperatures T_1 and T_2, first of all we recall that two temperatures, namely kinetic (T) and configurational (θ), have been used previously in the literature [15–17, 26–30] to describe aging and mechanical rejuvenation of amorphous solids, specifically [17]

$$T = \left.\frac{\delta U_{\rm em}}{\delta s}\right|_{\eta,\boldsymbol{F}}, \tag{17}$$

$$\theta = \left.\frac{\delta U_{\rm em}}{\delta \eta}\right|_{s,\boldsymbol{F}}, \tag{18}$$

with $U_{\rm em} = U_{\rm em}[s, \eta, \boldsymbol{F}]$ the internal energy of the elastomer matrix, and the kinetic (s) and configurational (η) entropy densities of the elastomer matrix, which add up to the total entropy density of the elastomer matrix $s_{\rm em} = s + \eta$. In the following, the relation between the temperature pairs (T, θ) and (T_1, T_2) is elaborated.

In the present study, in contrast to [17], the internal energy U and the entropy S depend on the filler-particle arrangement p. To proceed, we assume that

$$U = U_{\rm em}[s, \eta, \boldsymbol{F}] + U_{\rm p}[p], \tag{19}$$

in other words, there is an additive filler-particle contribution to the energy that is independent of the partial elastomer entropies s and η. Hence, the entropy-derivatives of U become

$$\left.\frac{\delta U}{\delta s}\right|_{\eta,\boldsymbol{F},p} = \left.\frac{\delta U_{\rm em}}{\delta s}\right|_{\eta,\boldsymbol{F}} = T, \tag{20}$$

$$\left.\frac{\delta U}{\delta \eta}\right|_{s,\boldsymbol{F},p} = \left.\frac{\delta U_{\rm em}}{\delta \eta}\right|_{s,\boldsymbol{F}} = \theta, \tag{21}$$

according to (17) and (18). Consideration of the change of variables $s \to s_{\rm t}$ implies that the internal energy U can be written in the form $U = U_{\rm em}[s(s_{\rm t}, \eta, s_{\rm p}), \eta, \boldsymbol{F}] + U_{\rm p}[p]$, with derivatives

$$T_1 = \left.\frac{\delta U}{\delta s_{\rm t}}\right|_{\eta,\boldsymbol{F},p} = \left.\frac{\delta U_{\rm em}[s, \eta, \boldsymbol{F}]}{\delta s}\right|_{\eta,\boldsymbol{F}} \left.\frac{\partial s}{\partial s_{\rm t}}\right|_{\eta,s_{\rm p}} = T, \tag{22}$$

$$T_2 = \left.\frac{\delta U}{\delta \eta}\right|_{s_{\rm t},\boldsymbol{F},p} = \left.\frac{\delta U_{\rm em}[s, \eta, \boldsymbol{F}]}{\delta s}\right|_{\eta,\boldsymbol{F}} \left.\frac{\partial s}{\partial \eta}\right|_{s_{\rm t},s_{\rm p}} + \left.\frac{\delta U_{\rm em}}{\delta \eta}\right|_{s,\boldsymbol{F}} = -T + \theta, \tag{23}$$

where we have again used the definitions (17) and (18) as well as the split, in complete analogy to (19),

$$s_{\rm t} = s + \eta + s_{\rm p}[p], \tag{24}$$

where the filler-particle entropy $s_{\rm p}$ does not depend on s and η. It should be noted, that in the expressions (22) and (23), constant p implies that $s_{\rm p}$ is constant, by virtue of (24). Equations (22) and (23) provide the desired physical interpretation of T_1 and T_2 defined in (15) and (16) by relating them to the kinetic and configurational temperatures, (17) and (18), respectively.

The assumptions (19) and (24) state that the filler-particle contributions to the internal energy and to the entropy do not depend on the thermodynamic state of the elastomer matrix. To support these assumptions, one can argue as follows. Using the assumptions (19) and (24), the temperatures T and θ, derived from (22) and (23), are functions $T = T(s, \eta, \boldsymbol{F})$, $\theta = \theta(s, \eta, \boldsymbol{F})$, from which one can obtain the inverse functions $s = s(T, \theta, \boldsymbol{F})$, $\eta = \eta(T, \theta, \boldsymbol{F})$. Substituting these into (19) and (24), one obtains

$$U = U_{\rm em}[T, \theta, \boldsymbol{F}] + U_{\rm p}[p], \tag{25}$$

$$S = S_{\rm em}[T, \theta, \boldsymbol{F}] + S_{\rm p}[p], \tag{26}$$

in terms of temperatures.

In the sequel, it is discussed under what circumstances the forms (25) and (26) for the energy U and the entropy S are the natural ones. In the most general case, the internal energy U and the entropy S are functionals of all dynamic variables. In practical applications, however, it is convenient to split these functionals additively into their elastomer-matrix and filler-particle contributions. Let us consider the potential Φ describing the energy stored in the system because of the current state $\boldsymbol{R}$ being different from the load-free state $\boldsymbol{Q}$. Since Φ plays the role of a Helmholtz free energy, it decomposes into energetic and entropic parts, $\Phi = \Phi^{\mathrm{E}} + \Phi^{\mathrm{S}}$ [5, 23] by way of

$$\Phi^{\mathrm{E}} = \Phi - T\frac{\partial \Phi}{\partial T}\,, \tag{27}$$

$$\Phi^{\mathrm{S}} = T\frac{\partial \Phi}{\partial T}\,. \tag{28}$$

For the case that the potential Φ depends linearly on temperature T, namely $\Phi = \Phi_0 + T\Phi_1$ with T-independent Φ_0 and Φ_1, one can readily see that $\Phi^{\mathrm{S}} = T\Phi_1$ and $\Phi^{\mathrm{E}} = \Phi_0$. For the p-dependent contribution U_{p} to the internal energy $U = U_{\mathrm{em}}[T, \theta, \boldsymbol{F}] + U_{\mathrm{p}}[p]$ and the p-dependent contribution S_{p} to the entropy $S = S_{\mathrm{em}}[T, \theta, \boldsymbol{F}] + S_{\mathrm{p}}[p]$, one thus finds

$$U_{\mathrm{p}}[p] = \iint p\Phi_0 d^6\boldsymbol{\xi} d^3\boldsymbol{r}\,, \tag{29}$$

$$S_{\mathrm{p}}[p] = -\iint p\Big(\Phi_1 + k_{\mathrm{B}} \ln p\Big) d^6\boldsymbol{\xi} d^3\boldsymbol{r}\,, \tag{30}$$

in agreement with (25) and (26), i.e. the filler-particle contributions U_{p} and S_{p} do not depend on the thermodynamic state of the elastomer matrix. This argument cannot only be used if $\Phi = \Phi_0 + T\Phi_1$ holds for the entire range of temperature, but also if this holds over a finite temperature range of interest.

In summary, the temperature-pairs (T, θ) and (T_1, T_2) have been related through (22) and (23). In what follows in this paper, we will work with T, θ rather than T_1, T_2, since the first set is more intuitive and relates to the previous studies [5] and [17].

3.3 Reversible dynamics

The reversible part of the dynamics of $\boldsymbol{\mathcal{X}}$, according to (2), is related to the gradient of energy $\delta E/\delta\boldsymbol{\mathcal{X}}$ (13) through the Poisson operator $\boldsymbol{\mathcal{L}}$. The reversible dynamics considered in this paper is all related to the deformation field, $\boldsymbol{v}(\boldsymbol{r})$. Inspection of the energy gradient (13) thus suggests that the determination of the Poisson operator should focus on the first column, and due to the anti-symmetry (5), the first row of $\boldsymbol{\mathcal{L}}$. To that end, one can depart from the model developed in [5] where the physical aging has not been included, and then add the configurational entropy η to that description in order to account for the physical aging. This leads to (see also [5, 17])

$$\boldsymbol{\mathcal{L}} = \begin{pmatrix} \mathcal{L}^{(mm)}_{\alpha\gamma} & \mathcal{L}^{(ms_{\mathrm{t}})}_{\alpha} & \mathcal{L}^{(m\eta)}_{\alpha} & \mathcal{L}^{(mF)}_{\alpha\gamma\varepsilon} & \mathcal{L}^{(mp)}_{\alpha} \\ \mathcal{L}^{(s_{\mathrm{t}}m)}_{\gamma} & 0 & 0 & 0 & 0 \\ \mathcal{L}^{(\eta m)}_{\gamma} & 0 & 0 & 0 & 0 \\ \mathcal{L}^{(Fm)}_{\alpha\beta\gamma} & 0 & 0 & 0 & 0 \\ \mathcal{L}^{(pm)}_{\gamma} & 0 & 0 & 0 & 0 \end{pmatrix}, \tag{31}$$

with the operators

$$\mathcal{L}^{(mm)}_{\alpha\gamma} = -\nabla^r_\gamma m_\alpha - m_\gamma \nabla^r_\alpha \,, \tag{32}$$
$$\mathcal{L}^{(ms_\mathrm{t})}_{\alpha} = -s_\mathrm{t} \nabla^r_\alpha \,, \tag{33}$$
$$\mathcal{L}^{(m\eta)}_{\alpha} = -\eta \nabla^r_\alpha \,, \tag{34}$$
$$\mathcal{L}^{(s_\mathrm{t}m)}_{\gamma} = -\nabla^r_\gamma s_\mathrm{t} \,, \tag{35}$$
$$\mathcal{L}^{(\eta m)}_{\gamma} = -\nabla^r_\gamma \eta, \tag{36}$$
$$\mathcal{L}^{(mF)}_{\alpha\gamma\varepsilon} = (\nabla^r_\alpha F_{\gamma\varepsilon}) + \nabla^r_\mu F_{\mu\varepsilon}\delta_{\alpha\gamma} \,, \tag{37}$$
$$\mathcal{L}^{(Fm)}_{\alpha\beta\gamma} = -\left(\nabla^r_\gamma F_{\alpha\beta}\right) + F_{\mu\beta}\nabla^r_\mu \delta_{\alpha\gamma} \,, \tag{38}$$
$$\mathcal{L}^{(mp)}_{\alpha} = -p'\nabla^r_\alpha + \nabla^r_\mu R'_\mu p' \nabla^{R'}_\alpha \,, \tag{39}$$
$$\mathcal{L}^{(pm)}_{\gamma} = -\nabla^r_\gamma p - \nabla^R_\gamma R_\mu p \nabla^r_\mu \,, \tag{40}$$

where f' stands for $f(\boldsymbol{\xi}')$ for any quantity f. It is emphasized that all differential operators, specifically ∇^r, ∇^R, and $\nabla^{R'}$ in (32)–(40), act on everything to their right, also on what will be multiplied to the right of $\boldsymbol{\mathcal{L}}$. The only exception to this rule is if the differential operator together with its object of action is enclosed in parenthesis. The same convention will be used in the remained of this paper, i.e. also in Sec. 3.4.

It should be pointed out that for the Poisson operator (31)–(40) both the degeneracy condition (4) and the anti-symmetry property (5) are satisfied. Moreover, the Jacobi identity (6) is satisfied as well, which can be proven as follows. In general, the Poisson operator in the Eulerian setting is induced by a Poisson operator in the Lagrangian setting [31]. Furthermore, it can be shown that the Jacobi identity in the Eulerian setting is guaranteed by the Jacobi identity in the Lagrangian setting. This result is useful here, since it is much easier to check the Jacobi identity in the Lagrangian setting, where the Poisson operator is almost trivial. Note that, with (36), it can be shown that the material time derivative (D_t) of the specific configurational entropy density, $\hat{\eta} = \eta/\rho$, is $D_t\hat{\eta} = 0$. Therefore, from a Lagrangian viewpoint, η does not participate in the reversible dynamics. With respect to the verification of the Jacobi identity, the case with variables (10) is thus identical with the one studied in [5], where the Jacobi identity has been found to be satisfied.

Having an explicit form for the Poisson operator, and multiplying it with the gradient of energy (13), one can write the reversible part (2) of the $\boldsymbol{\mathcal{X}}$-evolution equation in the form

$$\partial_t m_\alpha|_\mathrm{rev} = -\nabla^r_\gamma (m_\alpha v_\gamma) + \nabla^r_\gamma \hat{\sigma}_{\alpha\gamma} \,, \tag{41}$$
$$\partial_t s_\mathrm{t}|_\mathrm{rev} = -\nabla^r_\gamma (s_\mathrm{t} v_\gamma) \,, \tag{42}$$
$$\partial_t \eta|_\mathrm{rev} = -\nabla^r_\gamma (\eta v_\gamma) \,, \tag{43}$$
$$\partial_t F_{\alpha\beta}|_\mathrm{rev} = -v_\mu \left(\nabla^r_\mu F_{\alpha\beta}\right) + F_{\mu\beta}\left(\nabla^r_\mu v_\alpha\right) \,, \tag{44}$$
$$\partial_t p|_\mathrm{rev} = -\nabla^r_\gamma (p v_\gamma) - \nabla^R_\gamma \left(R_\mu p \left(\nabla^r_\mu v_\gamma\right)\right) \,, \tag{45}$$

with the stress-like quantity

$$\hat{\sigma}_{\alpha\gamma} = \left(u - Ts_\mathrm{t} - (\theta - T)\eta - \int p \left.\frac{\delta U}{\delta p}\right|_{s_\mathrm{t},\eta,\boldsymbol{F}} d^6\boldsymbol{\xi}\right)\delta_{\alpha\gamma} + \left.\frac{\delta U}{\delta F_{\alpha\varepsilon}}\right|_{s_\mathrm{t},\eta,p} F_{\gamma\varepsilon} + \int p R_\gamma \left(\nabla^R_\alpha \left.\frac{\delta U}{\delta p}\right|_{s_\mathrm{t},\eta,\boldsymbol{F}}\right) d^6\boldsymbol{\xi} \,, \tag{46}$$

as an extension of [5] with respect to the additional variable η. Here, u denotes the density of internal energy per unit volume, containing contributions of both the elastomer matrix and the filler particles. In view of (11), one therefore has $U = \int u\, d^3\boldsymbol{r}$. As will be discussed further below, the relation (46) is not yet the complete Cauchy stress tensor, particularly because the last particle-based contribution is not symmetric.

3.4 Irreversible dynamics

In this section, the irreversible contributions (3) to the $\boldsymbol{\mathcal{X}}$-evolution equations will be discussed. In view of [5,17], the irreversible dynamics can be split into dissipative and non-dissipative parts. Specifically the

viscoplastic deformation of glassy bridges [5] and physical aging of glassy material [17] enter as dissipative contributions to the dynamics, while non-affine deformation of the glassy network is represented by non-dissipative, but still irreversible, dynamics (see [5] for a detailed discussion on this latter point).

3.4.1 Dissipative part: Viscoplastic deformation and physical aging

In order to formulate the dissipative dynamics within the GENERIC framework, one starts from a factorization of the friction matrix [32]

$$\boldsymbol{\mathcal{M}} = \boldsymbol{\mathcal{C}}\boldsymbol{\mathcal{R}}\boldsymbol{\mathcal{C}}^* \,, \tag{47}$$

with a symmetric and positive semi-definite matrix $\boldsymbol{\mathcal{R}}$, the operator $\boldsymbol{\mathcal{C}}$ that represents the so-called mechanical part, and its adjoint operator $\boldsymbol{\mathcal{C}}^*$. Here and in what follows, the symbol $*$ stands for the adjoint operator. It is essential to note that the symmetry and positive semi-definiteness of $\boldsymbol{\mathcal{R}}$ automatically imply the corresponding conditions (8) and (9) for the friction matrix $\boldsymbol{\mathcal{M}}$. By requiring

$$\boldsymbol{\mathcal{C}}^* \frac{\delta E}{\delta \boldsymbol{\mathcal{X}}} = 0 \,, \tag{48}$$

the degeneracy condition (7) can be satisfied. It is emphasized that for these dissipative contributions to the dynamics, the Onsager-symmetry is relevant, i.e. (8) applies to $\boldsymbol{\mathcal{M}}$, and an analogous condition follows for $\boldsymbol{\mathcal{R}}$.

Since two different dissipative processes, i.e. viscoplastic deformation and physical aging of the glassy bridges, are to be modeled, one considers a matrix $\boldsymbol{\mathcal{R}}$ of rank two, and consequently $\boldsymbol{\mathcal{C}}$ and $\boldsymbol{\mathcal{C}}^*$ are 2×5 and 5×2 (generalized) matrices, respectively. The focus on these two dissipative processes implies that there will be two thermodynamic forces, denoted by $\boldsymbol{\mathcal{F}} = \left(\mathcal{F}^\Delta, \boldsymbol{\mathcal{F}}^p\right)$, and two corresponding thermodynamic fluxes, denoted by $\boldsymbol{\mathcal{J}} = \left(\mathcal{J}^\Delta, \boldsymbol{\mathcal{J}}^p\right)$ [23, 33].

If Newtonian viscous stresses are neglected, in analogy to [7], and since the total deformation gradient describes purely affine kinematics, the evolution equations of both $\boldsymbol{m}$ and $\boldsymbol{F}$ do not have any dissipative contributions. Therefore, it is reasonable to assume that the first and fourth rows of $\boldsymbol{\mathcal{C}}$, and therefore the first and fourth columns of $\boldsymbol{\mathcal{C}}^*$, must be zero. Hence, a reasonable ansatz for the operators $\boldsymbol{\mathcal{C}}$ and $\boldsymbol{\mathcal{C}}^*$ is given by

$$\boldsymbol{\mathcal{C}} = \begin{pmatrix} 0 & 0 \\ \left(\frac{1}{T} - \frac{1}{\theta}\right) & \mathcal{C}_\gamma^{(s_\mathrm{t})} \\ -\frac{1}{\theta} & \mathcal{C}_\gamma^{(\eta)} \\ 0 & 0 \\ 0 & \mathcal{C}_\gamma^{(p)} \end{pmatrix} \,, \quad \boldsymbol{\mathcal{C}}^* = \begin{pmatrix} 0 & \left(\frac{1}{T} - \frac{1}{\theta}\right) & -\frac{1}{\theta} & 0 & 0 \\ 0 & \mathcal{C}_\alpha^{*(s_\mathrm{t})} & \mathcal{C}_\alpha^{*(\eta)} & 0 & \mathcal{C}_\alpha^{*(p)} \end{pmatrix} \,. \tag{49}$$

The explicit form of the first row of $\boldsymbol{\mathcal{C}}^*$, and as consequence the first column of $\boldsymbol{\mathcal{C}}$, is motivated by [17] in order to obtain the thermodynamic driving force for physical aging, i.e. $\mathcal{F}^\Delta = (1/T - 1/\theta)$. More explicitly, the process of physical aging goes on until the configurational temperature θ approaches the kinetic temperature T, in which case the thermodynamic driving force $\mathcal{F}^\Delta$ vanishes. Moreover, the given form of the first row of $\boldsymbol{\mathcal{C}}^*$ satisfies the degeneracy condition (48).

In order to determine all other unknown elements of the operators $\boldsymbol{\mathcal{C}}$ and $\boldsymbol{\mathcal{C}}^*$, one starts with considering the evolution equation of the filler-particle arrangement p. While this has been studied in [5] in the absence of aging, that procedure is adapted in this paper to account for physical aging. In view of the Liouville theorem [34], the (irreversible part of the) evolution of p must have the form of the divergence of the thermodynamic flux, namely

$$\partial_t p(\boldsymbol{r}, \boldsymbol{\xi})|_\mathrm{diss} = \int \delta(\boldsymbol{R} - \boldsymbol{R}') \left(\nabla_\gamma^{Q'} \delta(\boldsymbol{Q} - \boldsymbol{Q}')\right) \mathcal{J}_\gamma^\mathrm{p}(\boldsymbol{\xi}')\, d^6\boldsymbol{\xi}' \,, \tag{50}$$

with the thermodynamic flux $\mathcal{J}_\gamma^\mathrm{p}$ for viscoplastic deformation. In view of the last row of $\boldsymbol{\mathcal{C}}$ and the equation (50), one can explicitly determine $\mathcal{C}_\gamma^{(p)}$ and its adjoint $\mathcal{C}_\alpha^{*(p)}$ [5],

$$\mathcal{C}_\gamma^{(p)} = \delta\left(\boldsymbol{R} - \boldsymbol{R}'\right) \left(\nabla_\gamma^{Q'} \delta\left(\boldsymbol{Q} - \boldsymbol{Q}'\right)\right) \,, \tag{51}$$

$$\mathcal{C}_\alpha^{*(p)} = \delta\left(\boldsymbol{R}' - \boldsymbol{R}\right) \left(\nabla_\alpha^{Q} \delta\left(\boldsymbol{Q}' - \boldsymbol{Q}\right)\right) \,. \tag{52}$$

Consequently, the degeneracy condition (48) applied to the second row of $\boldsymbol{\mathcal{C}}^*$ reads

$$\mathcal{C}_\alpha^{*(s_\mathrm{t})} T + \mathcal{C}_\alpha^{*(\eta)} (\theta - T) = - \left(\nabla_\alpha^Q \left. \frac{\delta U}{\delta p} \right|_{s_\mathrm{t}, \eta, \boldsymbol{F}} \right) . \tag{53}$$

This condition, however, does not give a unique solution for the operators $\mathcal{C}_\alpha^{*(s_\mathrm{t})}$ and $\mathcal{C}_\alpha^{*(\eta)}$, but rather needs to be supplemented by an extra assumption. An intuitive assumption is to adopt the case where both $\mathcal{C}_\alpha^{*(s_\mathrm{t})}$ and $\mathcal{C}_\alpha^{*(\eta)}$ are proportional to the right-hand side expression. Motivated by [17], where instead of the total entropy density as a dynamic variable the entropy density of the kinetic subsystem is used (rendering the description more "symmetric"), we choose the operators $\mathcal{C}_\alpha^{*(s_\mathrm{t})}$ and $\mathcal{C}_\alpha^{*(\eta)}$ to be of the form

$$\mathcal{C}_\alpha^{*(s_\mathrm{t})} = - \left(\frac{\varphi}{T} + \frac{(1-\varphi)}{\theta} \right) \left(\nabla_\alpha^Q \left. \frac{\delta U}{\delta p} \right|_{s_\mathrm{t}, \eta, \boldsymbol{F}} \right) , \tag{54}$$

$$\mathcal{C}_\alpha^{*(\eta)} = - \frac{(1-\varphi)}{\theta} \left(\nabla_\alpha^Q \left. \frac{\delta U}{\delta p} \right|_{s_\mathrm{t}, \eta, \boldsymbol{F}} \right) , \tag{55}$$

with an arbitrary function $\varphi(\boldsymbol{\mathcal{X}})$. This specific choice satisfies the degeneracy condition (53), and it switches off either the T- or the θ-contributions to $\mathcal{C}_\alpha^{*(s_\mathrm{t})}$ and $\mathcal{C}_\alpha^{*(\eta)}$ for $\varphi = 0$ or $\varphi = 1$, respectively, in analogy to [17]. Making use of the symmetry-condition of $\boldsymbol{\mathcal{M}}$ leads to

$$\mathcal{C}_\gamma^{(s_\mathrm{t})} = - \left(\frac{\varphi'}{T} + \frac{(1-\varphi')}{\theta} \right) \left(\nabla_\gamma^{Q'} \left. \frac{\delta U}{\delta p'} \right|_{s_\mathrm{t}, \eta, \boldsymbol{F}} \right) , \tag{56}$$

$$\mathcal{C}_\gamma^{(\eta)} = - \frac{(1-\varphi')}{\theta} \left(\nabla_\gamma^{Q'} \left. \frac{\delta U}{\delta p'} \right|_{s_\mathrm{t}, \eta, \boldsymbol{F}} \right) . \tag{57}$$

At this point, we have determined the operators $\boldsymbol{\mathcal{C}}$ and $\boldsymbol{\mathcal{C}}^*$, and therefore one can calculate the thermodynamic driving forces for physical aging ($\mathcal{F}^\Delta$) and viscoplastic deformation of the glassy bridges ($\boldsymbol{\mathcal{F}}^p$), namely

$$\mathcal{F}^\Delta = \frac{1}{T} - \frac{1}{\theta} \tag{58}$$

$$\boldsymbol{\mathcal{F}}^p = - \left(\frac{\varphi}{T} + \frac{(1-\varphi)}{\theta} \right) \left(\nabla_\alpha^Q \left. \frac{\delta U}{\delta p} \right|_{s_\mathrm{t}, \eta, \boldsymbol{F}} \right) . \tag{59}$$

To obtain the thermodynamic flux $\boldsymbol{\mathcal{J}}$, first of all we use the decomposition $\boldsymbol{\mathcal{R}} = \boldsymbol{\mathcal{R}}^\mathrm{x} + \boldsymbol{\mathcal{R}}^\mathrm{p}$, with contributions representative of the exchange between the kinetic and configurational subsystems ("x") for the process of physical aging, and of viscoplastic deformation ("p") of the glassy bridges. Motivated by [17], one can express the operator $\boldsymbol{\mathcal{R}}^\mathrm{x}$ in the following form

$$\boldsymbol{\mathcal{R}}^\mathrm{x} = \begin{pmatrix} \mu^\mathrm{x} & 0 \\ 0 & 0 \end{pmatrix} , \tag{60}$$

with $\mu^\mathrm{x} \geq 0$, which leads to the flux $\boldsymbol{\mathcal{J}}^\mathrm{x} = \boldsymbol{\mathcal{R}}^\mathrm{x} \boldsymbol{\mathcal{F}} = (\mathcal{J}^{\Delta,\mathrm{x}}, 0)$ with

$$\mathcal{J}^{\Delta,\mathrm{x}} = \mu^\mathrm{x} \mathcal{F}^\Delta = \mu^\mathrm{x} \left(\frac{1}{T} - \frac{1}{\theta} \right) . \tag{61}$$

Next, the formulation of viscoplastic deformation of the glassy bridges is considered. Since the driving force $\boldsymbol{\mathcal{F}}^p$ in (59) contains a term proportional to $(1/T - 1/\theta)$ as does $\mathcal{F}^\Delta$ in (58), one needs to allow in principle for a combination of both $\mathcal{F}^\Delta$ and $\boldsymbol{\mathcal{F}}^p$ to obtain the effective driving force for viscoplastic deformation, similarly to [17], which can be represented by

$$\boldsymbol{\mathcal{R}}^\mathrm{p} = \begin{pmatrix} \omega_\mu(\boldsymbol{\xi}) \\ \delta_{\alpha\mu} \end{pmatrix} \lambda_{\mu\nu}(\boldsymbol{\xi}, \boldsymbol{\xi}') \begin{pmatrix} \omega_\nu(\boldsymbol{\xi}') & \delta_{\nu\gamma} \end{pmatrix} , \tag{62}$$

where the symmetry and positive semi-definiteness of $\boldsymbol{\mathcal{R}}^{\mathrm{p}}$ requires the same for $\lambda_{\mu\nu}$. With the ansatz (62), one can determine the fluxes, related to viscoplastic deformation, namely $\boldsymbol{\mathcal{J}}^{\mathrm{p}} = \boldsymbol{\mathcal{R}}^{\mathrm{p}}\boldsymbol{\mathcal{F}} = (\mathcal{J}^{\Delta,\mathrm{p}}, \boldsymbol{\mathcal{J}}^{p,\mathrm{p}})$ with

$$\mathcal{J}^{\Delta,\mathrm{p}} = \omega_\mu \mathcal{J}_\mu^{p,\mathrm{p}}\,, \tag{63}$$

$$\mathcal{J}_\alpha^{p,\mathrm{p}}(\boldsymbol{\xi}) = \int \lambda_{\alpha\nu}(\boldsymbol{\xi},\boldsymbol{\xi}')\mathcal{F}_\nu^{p,\mathrm{eff}}(\boldsymbol{\xi}')\,d^6\boldsymbol{\xi}'\,, \tag{64}$$

with the effective driving force

$$\mathcal{F}_\alpha^{p,\mathrm{eff}} = \omega_\alpha \mathcal{F}^\Delta + \mathcal{F}_\alpha^p\,. \tag{65}$$

Equation (63) relates the effective driving force to the current density in the filler-particle arrangement space. Furthermore, relations (63) and (64) show that ω_α plays a twofold role. On the one hand it enters the effective driving force (65). On the other hand, it leads to a non-zero contribution to the exchange between the kinetic and configurational subsystems, (63), due to viscoplastic deformation. As will be discussed below, the quantity ω_α will become essential for modeling the so-called mechanical rejuvenation of the glassy bridges, i.e., the fluidization of the glassy bridges due to the applied load, thereby affecting the macroscopic mechanical response of the entire nanocomposite. The mechanical rejuvenation of bulk glassy polymers has been studied in detail, both experimentally [35,36] as well as in modeling and simulation [15,16], and it has also been incorporated previously in nanocomposite models in a non-thermodynamic manner [8,9].

Finally, collecting all dissipative contributions discussed above, the corresponding contributions to the evolution equations of $\boldsymbol{\mathcal{X}}$ become

$$\partial_t m_\alpha|_{\mathrm{diss}} = 0\,, \tag{66}$$

$$\partial_t s_{\mathrm{t}}|_{\mathrm{diss}} = \left(\frac{1}{T}-\frac{1}{\theta}\right)\mathcal{J}^{\Delta,\mathrm{x}} + \left(\frac{1}{T}-\frac{1}{\theta}\right)\int \mathcal{J}^{\Delta,\mathrm{p}}\,d^6\boldsymbol{\xi} - \int\left(\frac{\varphi}{T}+\frac{(1-\varphi)}{\theta}\right)\left(\nabla_\gamma^Q\,\frac{\delta U}{\delta p}\bigg|_{s_{\mathrm{t}},\eta,\boldsymbol{F}}\right)\mathcal{J}_\gamma^{p,\mathrm{p}}\,d^6\boldsymbol{\xi}\,, \tag{67}$$

$$\partial_t \eta|_{\mathrm{diss}} = -\frac{1}{\theta}\mathcal{J}^{\Delta,\mathrm{x}} - \frac{1}{\theta}\int \mathcal{J}^{\Delta,\mathrm{p}} d^6\boldsymbol{\xi} - \int\frac{(1-\varphi)}{\theta}\left(\nabla_\gamma^Q\,\frac{\delta U}{\delta p}\bigg|_{s_{\mathrm{t}},\eta,\boldsymbol{F}}\right)\mathcal{J}_\gamma^{p,\mathrm{p}}\,d^6\boldsymbol{\xi}\,, \tag{68}$$

$$\partial_t F_{\alpha\beta}|_{\mathrm{diss}} = 0\,, \tag{69}$$

$$\partial_t p|_{\mathrm{diss}} = -\nabla_\gamma^Q\,\mathcal{J}_\gamma^{p,\mathrm{p}}\,, \tag{70}$$

with the thermodynamic fluxes $\mathcal{J}^{\Delta,\mathrm{x}}$, $\mathcal{J}^{\Delta,\mathrm{p}}$ and $\mathcal{J}_\gamma^{p,\mathrm{p}}$, given by the expressions (61) and (63)–(64), respectively. The set of equations (66)–(70) clearly shows the effects of heat exchange between the two thermal subsystems ("x") representative of physical aging, and of viscoplastic deformation ("p").

3.4.2 Non-dissipative part: Non-affine deformation

Finally, let us discuss the irreversible but non-dissipative contributions to the evolution of $\boldsymbol{\xi}$. In complete analogy to [5], the only reason to include such contributions is the observation that the stress-like quantity (46) is not symmetric in general, e.g. if $\nabla^R(\delta U/\delta p)$ is proportional to $\boldsymbol{R}-\boldsymbol{Q}$ (see below). However, it was argued in [5] that the symmetry of the stress tensor can indeed be restored by excluding the anti-symmetric part of the imposed velocity gradient from the last contribution to the p-evolution equation (45). It is pointed out that, in contrast to the dissipative dynamics discussed in Sec. 3.4.1, in this section the Onsager-symmetry (8) must be replaced by the Casimir-symmetry, namely $\boldsymbol{\mathcal{M}}^{\mathrm{T}} = -\boldsymbol{\mathcal{M}}$, leading to the absence of dissipation. The reader is referred to [23] for the conceptual details on this issue, and for an example in complex fluids modeling.

To exclude the anti-symmetric part of the imposed velocity gradient from the last contribution to the p-evolution equation (45), the following contribution to its evolution needs to be added [5],

$$\partial_t p|_{\mathrm{non-a}} = -\nabla_\nu^R\left(\frac{1}{2}\left[(\nabla_\nu^r v_\mu) - \left(\nabla_\mu^r v_\nu\right)\right]R_\mu p\right)\,. \tag{71}$$

As an extension to the case studied in [5], we consider the irreversible but non-dissipative operator $\tilde{\boldsymbol{\mathcal{M}}}$ of the form

$$\tilde{\boldsymbol{\mathcal{M}}} = \begin{pmatrix} 0 & \tilde{\mathcal{M}}_\alpha^{(ms_\mathrm{t})} & \tilde{\mathcal{M}}_\alpha^{(m\eta)} & 0 & \tilde{\mathcal{M}}_\alpha^{(mp)} \\ \tilde{\mathcal{M}}_\gamma^{(s_\mathrm{t}m)} & 0 & 0 & 0 & \tilde{\mathcal{M}}^{(s_\mathrm{t}p)} \\ \tilde{\mathcal{M}}_\gamma^{(\eta m)} & 0 & 0 & 0 & \tilde{\mathcal{M}}^{(\eta p)} \\ 0 & 0 & 0 & 0 & 0 \\ \tilde{\mathcal{M}}_\gamma^{(pm)} & \tilde{\mathcal{M}}^{(ps_\mathrm{t})} & \tilde{\mathcal{M}}^{(p\eta)} & 0 & 0 \end{pmatrix}, \tag{72}$$

where the structure of the third row is such, that the configurational entropy density of the elastomer, η, is not altered, similarly to s_t. In view of the specific form of $\tilde{\boldsymbol{\mathcal{M}}}$ and the entropy gradient (14), one can uniquely determine $\tilde{\boldsymbol{\mathcal{M}}}^{(ps_\mathrm{t})}$,

$$\tilde{\mathcal{M}}^{(ps_\mathrm{t})} = -\frac{1}{2}\left(\nabla_\nu^R R_\mu p\right)\left[(\nabla_\nu^r v_\mu) - \left(\nabla_\mu^r v_\nu\right)\right], \tag{73}$$

in order to reproduce (71) [5]. Subsequently applying the degeneracy condition (7) to the last row of $\tilde{\boldsymbol{\mathcal{M}}}$ leads to

$$\tilde{\mathcal{M}}_\gamma^{(pm)} v_\gamma + \tilde{\mathcal{M}}^{(ps_\mathrm{t})} T + \tilde{\mathcal{M}}^{(p\eta)}(\theta - T) = 0\,. \tag{74}$$

Requiring the same structure for $\tilde{\mathcal{M}}^{(ps_\mathrm{t})}$ and $\tilde{\mathcal{M}}^{(p\eta)}$, and consequently for $\tilde{\mathcal{M}}_\gamma^{(pm)} v_\gamma$, one finds

$$\tilde{\mathcal{M}}_\gamma^{(pm)} = \frac{1}{2}\left(\nabla_\nu^R R_\mu p\right)\left(T + (\theta - T)\zeta\right)\left[\delta_{\gamma\mu}\nabla_\nu^r - \delta_{\gamma\nu}\nabla_\mu^r\right], \tag{75}$$

$$\tilde{\mathcal{M}}^{(p\eta)} = -\frac{1}{2}\left(\nabla_\nu^R R_\mu p\right)\zeta\left[(\nabla_\nu^r v_\mu) - \left(\nabla_\mu^r v_\nu\right)\right], \tag{76}$$

with an arbitrary function ζ of the variables $\boldsymbol{\mathcal{X}}$, $\zeta(\boldsymbol{\mathcal{X}})$. In order to obtain the operator $\tilde{\mathcal{M}}^{(s_\mathrm{t}p)}$, we make use of the Casimir-symmetry condition, applied to (73), which results in

$$\tilde{\mathcal{M}}^{(s_\mathrm{t}p)} = \frac{1}{2}\left(\nabla_\nu^{R'} R'_\mu p'\right)\left[(\nabla_\nu^r v_\mu) - \left(\nabla_\mu^r v_\nu\right)\right], \tag{77}$$

$$\tilde{\mathcal{M}}_\gamma^{(s_\mathrm{t}m)} = -\frac{1}{2}\int \left.\frac{\delta U}{\delta p}\right|_{s_\mathrm{t},\eta,\boldsymbol{F}} \left(\nabla_\nu^R R_\mu p\right) d^6\boldsymbol{\xi}\left[\delta_{\gamma\mu}\nabla_\nu^r - \delta_{\gamma\nu}\nabla_\mu^r\right], \tag{78}$$

where (78) was obtained by using the degeneracy condition (7). Further, using again the Casimir-symmetry for (76) followed by the the degeneracy condition (7), one obtains

$$\tilde{\mathcal{M}}^{(\eta p)} = \frac{1}{2}\left(\nabla_\nu^{R'} R'_\mu p'\right)\zeta'\left[(\nabla_\nu^r v_\mu) - \left(\nabla_\mu^r v_\nu\right)\right], \tag{79}$$

$$\tilde{\mathcal{M}}_\gamma^{(\eta m)} = -\frac{1}{2}\int \left.\frac{\delta U}{\delta p}\right|_{s_\mathrm{t},\eta,\boldsymbol{F}} \left(\nabla_\nu^R R_\mu p\right)\zeta\, d^6\boldsymbol{\xi}\left[\delta_{\gamma\mu}\nabla_\nu^r - \delta_{\gamma\nu}\nabla_\mu^r\right]. \tag{80}$$

Finally, applying the Casimir-symmetry condition to (78), (80) and (75), the remaining elements of $\boldsymbol{\mathcal{M}}$ can be determined,

$$\tilde{\mathcal{M}}_\alpha^{(ms_\mathrm{t})} = -\frac{1}{2}\left[\delta_{\alpha\mu}\nabla_\nu^r - \delta_{\alpha\nu}\nabla_\mu^r\right]\int \left.\frac{\delta U}{\delta p}\right|_{s_\mathrm{t},\eta,\boldsymbol{F}} \left(\nabla_\nu^R R_\mu p\right) d^6\boldsymbol{\xi}\,, \tag{81}$$

$$\tilde{\mathcal{M}}_\alpha^{(m\eta)} = -\frac{1}{2}\left[\delta_{\alpha\mu}\nabla_\nu^r - \delta_{\alpha\nu}\nabla_\mu^r\right]\int \zeta\left.\frac{\delta U}{\delta p}\right|_{s_\mathrm{t},\eta,\boldsymbol{F}} \left(\nabla_\nu^R R_\mu p\right) d^6\boldsymbol{\xi}\,, \tag{82}$$

$$\tilde{\mathcal{M}}_\alpha^{(mp)} = \frac{1}{2}\left[\delta_{\alpha\mu}\nabla_\nu^r - \delta_{\alpha\nu}\nabla_\mu^r\right]\left(T + (\theta - T)\zeta'\right)\left(\nabla_\nu^{R'} R'_\mu p'\right). \tag{83}$$

It can be shown that the first row of the matrix $\tilde{\boldsymbol{\mathcal{M}}}$ complies with the degeneracy condition (7), which completes the procedure of determining $\tilde{\boldsymbol{\mathcal{M}}}$.

Summarizing the above, the contribution of non-affine dynamics to the evolution equations of $\boldsymbol{\mathcal{X}}$ can be written in the form

$$\partial_t m_\alpha|_{\text{non-a}} = \frac{1}{2}\nabla^r_\gamma \left[\int pR_\alpha \left(\nabla^R_\gamma \left. \frac{\delta U}{\delta p} \right|_{s_\text{t},\eta,\boldsymbol{F}} \right) d^6\boldsymbol{\xi} - \int pR_\gamma \left(\nabla^R_\alpha \left. \frac{\delta U}{\delta p} \right|_{s_\text{t},\eta,\boldsymbol{F}} \right) d^6\boldsymbol{\xi} \right] , \tag{84}$$

$$\partial_t s_\text{t}|_{\text{non-a}} = 0 , \tag{85}$$

$$\partial_t \eta|_{\text{non-a}} = 0 , \tag{86}$$

$$\partial_t F_{\alpha\beta}|_{\text{non-a}} = 0 , \tag{87}$$

$$\partial_t p|_{\text{non-a}} = -\frac{1}{2}\left(\nabla^R_\nu R_\mu p\right)\left[\left(\nabla^r_\nu v_\mu\right) - \left(\nabla^r_\mu v_\nu\right)\right] . \tag{88}$$

It can be seen from (85) that the total entropy of the system is not affected by these irreversible contributions, i.e. that the non-affine deformation implemented above is indeed free of dissipation.

3.5 Final set of evolution equations

3.5.1 Entropy-based formulation

The complete set of evolution equations for $\boldsymbol{\mathcal{X}}$, (1), is obtained by adding the reversible contributions discussed in Sec. 3.3 and the irreversible contributions discussed in Sec. 3.4.1 and Sec. 3.4.2, which leads to

$$\partial_t m_\alpha = -\nabla^r_\gamma \left(m_\alpha v_\gamma\right) + \nabla^r_\gamma \sigma_{\alpha\gamma} , \tag{89}$$

$$\begin{aligned} \partial_t s_\text{t} = {} & -\nabla^r_\gamma \left(s_\text{t} v_\gamma\right) + \left(\frac{1}{T} - \frac{1}{\theta}\right) \mathcal{J}^{\Delta,\text{x}} + \left(\frac{1}{T} - \frac{1}{\theta}\right) \int \mathcal{J}^{\Delta,\text{p}}\, d^6\boldsymbol{\xi} \\ & - \int \left(\frac{\varphi}{T} + \frac{(1-\varphi)}{\theta}\right) \left(\nabla^Q_\gamma \left. \frac{\delta U}{\delta p} \right|_{s_\text{t},\eta,\boldsymbol{F}} \right) \mathcal{J}^{p,\text{p}}_\gamma\, d^6\boldsymbol{\xi} , \end{aligned} \tag{90}$$

$$\partial_t \eta = -\nabla^r_\gamma \left(\eta v_\gamma\right) - \frac{1}{\theta}\mathcal{J}^{\Delta,\text{x}} - \frac{1}{\theta}\int \mathcal{J}^{\Delta,\text{p}}\, d^6\boldsymbol{\xi} - \int \frac{(1-\varphi)}{\theta} \left(\nabla^Q_\gamma \left. \frac{\delta U}{\delta p} \right|_{s_\text{t},\eta,\boldsymbol{F}} \right) \mathcal{J}^{p,\text{p}}_\gamma\, d^6\boldsymbol{\xi} , \tag{91}$$

$$\partial_t F_{\alpha\beta} = -v_\mu \left(\nabla^r_\mu F_{\alpha\beta}\right) + F_{\mu\beta}\left(\nabla^r_\mu v_\alpha\right) , \tag{92}$$

$$\partial_t p = -\nabla^r_\gamma \left(p v_\gamma\right) - \nabla^R_\gamma \left(pR_\mu \left[\nabla^r_\mu v_\gamma\right]^{\text{sym}} \right) - \nabla^Q_\gamma \mathcal{J}^{p,\text{p}}_\gamma , \tag{93}$$

with the stress tensor

$$\begin{aligned} \sigma_{\alpha\gamma} = {} & \left(u - Ts_\text{t} - (\theta - T)\eta - \int p \left. \frac{\delta U}{\delta p} \right|_{s_\text{t},\eta,\boldsymbol{F}} d^6\boldsymbol{\xi} \right) \delta_{\alpha\gamma} + \left. \frac{\delta U}{\delta F_{\alpha\varepsilon}} \right|_{s_\text{t},\eta,p} F_{\gamma\varepsilon} \\ & + \int \left[pR_\gamma \left(\nabla^R_\alpha \left. \frac{\delta U}{\delta p} \right|_{s_\text{t},\eta,\boldsymbol{F}} \right) \right]^{\text{sym}} d^6\boldsymbol{\xi} , \end{aligned} \tag{94}$$

and thermodynamic fluxes $\mathcal{J}^{\Delta,\text{x}}$, $\mathcal{J}^{\Delta,\text{p}}$ and $\mathcal{J}^{p,\text{p}}_\gamma$, given by (61), (63) and (64), respectively.

The Cauchy stress tensor (94) consists of (i) an isotropic pressure contribution due to both the elastomer matrix and the glassy network (first term on the right-hand side (r.h.s.)), (ii) a conventional anisotropic contribution of the elastomer matrix (second term), and (iii) an anisotropic contribution of the glassy network (third term). The latter is in agreement with statistical mechanics results [37–39] and formally corresponds to what is used in polymer kinetic theory [23, 40, 41]. For the case of thermal equilibrium, i.e. $\theta = T$ after long aging, this expression reduces to the one in [5]. Finally, it is noted that the Cauchy stress tensor (94) is manifestly symmetric.

3.5.2 Temperature-based formulation

The choice of the total entropy density s_t and the elastomer configurational entropy density η as dynamic variables is convenient from a fundamental model-development viewpoint. In practical applications, however, it is more convenient to work with temperatures. To that end, one must re-express the expressions

for the $\boldsymbol{F}$- and p-derivatives of U, as well as the time-evolution of the entropies s_t and η when using other dynamic variables than (s_t,η). Under a transformation of variables $(\boldsymbol{m},s_\mathrm{t},\eta,\boldsymbol{F},p)\rightarrow(\boldsymbol{m},T,\theta,\boldsymbol{F},p)$, the internal energy becomes a functional of the form $U=U[s_\mathrm{t}[T,\theta,\boldsymbol{F},p],\eta(T,\theta,\boldsymbol{F}),\boldsymbol{F},p]$. For thermodynamic functions of the form (19) and (24), or (25) and (26), respectively, one can show that derivatives of U with respect to $\boldsymbol{F}$ and p become

$$\left.\frac{\delta U}{\delta F_{\gamma\varepsilon}}\right|_{s_\mathrm{t},\eta,p} = \left.\frac{\delta U}{\delta F_{\gamma\varepsilon}}\right|_{T,\theta,p} - T\left.\frac{\delta(S_\mathrm{em}-H)}{\delta F_{\gamma\varepsilon}}\right|_{T,\theta} - \theta\left.\frac{\delta H}{\delta F_{\gamma\varepsilon}}\right|_{T,\theta}, \tag{95}$$

$$\left.\frac{\delta U}{\delta p}\right|_{s_\mathrm{t},\eta,\boldsymbol{F}} = \left.\frac{\delta U}{\delta p}\right|_{T,\theta,\boldsymbol{F}} - T\left.\frac{\delta S}{\delta p}\right|_{T,\theta,\boldsymbol{F}}, \tag{96}$$

with $H=\int\eta\,d^3\boldsymbol{r}$. Therefore, when translating the dynamic model from an entropy-based formulation to a temperature-based formulation, all occurrences of the derivatives on the left-hand side (l.h.s.) of (95) and (96) need to be replaced by their corresponding counter-parts on the r.h.s. of (95) and (96), respectively.

The expression (95) can be rationalized as follows: In terms of the variables $(T,\theta,\boldsymbol{F},p)$, both the internal energy U as well as the two partial entropies (kinetic and configurational) of the elastomer matrix, $S_\mathrm{em}-H$ and H, depend on $\boldsymbol{F}$. These entropy contributions are combined with the internal energy by pre-multiplying them with the respective (kinetic and configurational) temperature, similar to the expression for a Helmholtz free energy. In contrast, in (96), the p-dependent contributions of both the internal energy and the entropy are linked to neither the kinetic nor the configurational subsystems of the elastomer matrix, and one might hence wonder how to combine the p-derivatives of the energy and the entropy with each other. To that end, as the derivation of (96) also shows, the relevant factor is the functional derivative of the internal energy U with respect to s_t, which is in the first place equal to T_1. For the special form of thermodynamic potentials considered in this paper, Sec. 3.2, T_1 is equal to the kinetic temperature of the elastomer matrix, T. In this sense, the expression (96) is not as asymmetric with respect to the kinetic/configurational subsystems as it might seem on first sight.

The time-evolution of s_t and η can be reformulated by remembering that $S=S_\mathrm{em}[T,\theta,\boldsymbol{F}]+S_\mathrm{p}[p]$ and $H=H[T,\theta,\boldsymbol{F}]$, leading to

$$\partial_t s_\mathrm{t} = \left.\frac{\partial s_\mathrm{em}}{\partial T}\right|_{\theta,\boldsymbol{F}}\partial_t T + \left.\frac{\partial s_\mathrm{em}}{\partial\theta}\right|_{T,\boldsymbol{F}}\partial_t\theta + \left.\frac{\partial s_\mathrm{em}}{\partial F_{\gamma\varepsilon}}\right|_{T,\theta}\partial_t F_{\gamma\varepsilon} + \int\frac{\delta S_\mathrm{p}}{\delta p}\,\partial_t p\,d^6\boldsymbol{\xi}\,, \tag{97}$$

$$\partial_t\eta = \left.\frac{\partial\eta}{\partial T}\right|_{\theta,\boldsymbol{F}}\partial_t T + \left.\frac{\partial\eta}{\partial\theta}\right|_{T,\boldsymbol{F}}\partial_t\theta + \left.\frac{\partial\eta}{\partial F_{\gamma\varepsilon}}\right|_{T,\theta}\partial_t F_{\gamma\varepsilon}\,. \tag{98}$$

Substituting all the ingredients above, namely (95), (96), (97) and (98), into the evolution equations for s_t and η, results in

$$\begin{aligned} s_{\mathrm{em},T}D_tT + s_{\mathrm{em},\theta}D_t\theta = {}& \left[\left(-s_\mathrm{t}+\int\frac{\delta S_\mathrm{p}}{\delta p}\,p\,d^6\boldsymbol{\xi}\right)\delta_{\gamma\mu} - \left.\frac{\partial s_\mathrm{em}}{\partial F_{\gamma\varepsilon}}\right|_{T,\theta}F_{\mu\varepsilon}\right. \\ & - \left.\int p\left[R_\mu\left(\nabla^R_\gamma\frac{\delta S_\mathrm{p}}{\delta p}\right)\right]^{\mathrm{sym}}d^6\boldsymbol{\xi}\right]\left(\nabla^r_\mu v_\gamma\right) + \int\frac{\delta S_\mathrm{p}}{\delta p}\left(\nabla^Q_\gamma\mathcal{J}^{p,\mathrm{p}}_\gamma\right)d^6\boldsymbol{\xi} + \left(\frac{1}{T}-\frac{1}{\theta}\right)\mathcal{J}^{\Delta,\mathrm{x}} \\ & + \left(\frac{1}{T}-\frac{1}{\theta}\right)\int\mathcal{J}^{\Delta,\mathrm{p}}\,d^6\boldsymbol{\xi} - \int\left(\frac{\varphi}{T}+\frac{(1-\varphi)}{\theta}\right)\left[\nabla^Q_\gamma\left(\left.\frac{\delta U}{\delta p}\right|_{T,\theta,\boldsymbol{F}} - T\left.\frac{\delta S}{\delta p}\right|_{T,\theta,\boldsymbol{F}}\right)\right]\mathcal{J}^{p,\mathrm{p}}_\gamma d^6\boldsymbol{\xi}\,, \end{aligned} \tag{99}$$

$$\begin{aligned} \eta_{,T}D_tT + \eta_{,\theta}D_t\theta = {}& \left(-\eta\delta_{\gamma\mu} - \left.\frac{\partial\eta}{\partial F_{\gamma\varepsilon}}\right|_{T,\theta}F_{\mu\varepsilon}\right)\left(\nabla^r_\mu v_\gamma\right) - \frac{1}{\theta}\mathcal{J}^{\Delta,\mathrm{x}} \\ & - \frac{1}{\theta}\int\mathcal{J}^{\Delta,\mathrm{p}}\,d^6\boldsymbol{\xi} - \int\frac{(1-\varphi)}{\theta}\left[\nabla^Q_\gamma\left(\left.\frac{\delta U}{\delta p}\right|_{T,\theta,\boldsymbol{F}} - T\left.\frac{\delta S}{\delta p}\right|_{T,\theta,\boldsymbol{F}}\right)\right]\mathcal{J}^{p,\mathrm{p}}_\gamma d^6\boldsymbol{\xi}\,, \end{aligned} \tag{100}$$

with $D_t=\partial_t+v_\gamma\nabla^r_\gamma$ the substantial (material) time-derivative, and with the abbreviations

$$s_{\mathrm{em},T} = \left.\frac{\partial s_\mathrm{em}}{\partial T}\right|_{\theta,\boldsymbol{F}}, \quad s_{\mathrm{em},\theta} = \left.\frac{\partial s_\mathrm{em}}{\partial\theta}\right|_{T,\boldsymbol{F}}, \quad \eta_{,T} = \left.\frac{\partial\eta}{\partial T}\right|_{\theta,\boldsymbol{F}}, \quad \eta_{,\theta} = \left.\frac{\partial\eta}{\partial\theta}\right|_{T,\boldsymbol{F}}. \tag{101}$$

In summary, the entropy-based model formulated in Sec. 3.5.1 takes the following form when formulated in terms of temperatures. The momentum balance (89) remains valid. The entropy evolution equations (90) and (91) are replaced by (99) and (100), while the evolution equations for the deformation gradient (92) and for the filler-particle arrangement (93) remain unchanged. In all of this, specifically in the stress tensor $\sigma_{\alpha\gamma}$ (94) and the thermodynamic flux contributions $\mathcal{J}^{\Delta,\mathrm{x}}$, $\mathcal{J}^{\Delta,\mathrm{p}}$, $\mathcal{J}^{p,\mathrm{p}}_\gamma$ given by (61), (63), (64), respectively, the functional derivatives with respect to $\boldsymbol{F}$ and p are subject to the replacements (95) and (96).

4 Specific system realization

4.1 Reduction on the level of evolution equations

In the procedure above, the model is formulated in terms of (i) evolution equations (89)–(93) or its equivalent temperature-formulation, (ii) the constitutive expression for the Cauchy stress tensor (94), and (iii) the thermodynamic fluxes (61), (63), (64). To make this model material specific, choices need to be made for the internal energy U and entropy S, the kinetic functions $\lambda_{\alpha\beta}$ and μ^{x}, and the functions φ and ω_α.

For illustration purposes, several assumptions will be made to simplify the model. Particularly, it is assumed that the interaction of the two thermal subsystems, kinetic and configurational, of the glassy elastomer material is negligibly small. This implies that each subsystem entropy does not depend on the temperature of the other subsystem [15,16]. Based on this, one can show that the temperature evolution equations (99) and (100) can be written in the form

$$\begin{aligned} s_{,T}\, D_t T &= \left[\left(-s - s_{\mathrm{p}}[p] + \int \frac{\delta S_{\mathrm{p}}}{\delta p}\, p\, d^6\boldsymbol{\xi}\right)\delta_{\gamma\mu} - \left.\frac{\partial s}{\partial F_{\gamma\varepsilon}}\right|_{T,\theta} F_{\mu\varepsilon} - \int p\left[R_\mu\left(\nabla^R_\gamma \frac{\delta S_{\mathrm{p}}}{\delta p}\right)\right]^{\mathrm{sym}} d^6\boldsymbol{\xi}\right](\nabla^r_\mu v_\gamma) \\ &\quad + \frac{1}{T}\mu^{\mathrm{x}}\left(\frac{1}{T}-\frac{1}{\theta}\right) + \frac{1}{T}\int\left(\breve{\omega}_\gamma - \left(\nabla^Q_\gamma \frac{\delta U_{\mathrm{p}}}{\delta p}\right)\right)\mathcal{J}^{p,\mathrm{p}}_\gamma d^6\boldsymbol{\xi}\,, \end{aligned} \tag{102}$$

$$\eta_{,\theta}\, D_t\theta = \left(-\eta\delta_{\gamma\mu} - \left.\frac{\partial \eta}{\partial F_{\gamma\varepsilon}}\right|_{T,\theta} F_{\mu\varepsilon}\right)(\nabla^r_\mu v_\gamma) - \frac{1}{\theta}\mu^{\mathrm{x}}\left(\frac{1}{T}-\frac{1}{\theta}\right) - \frac{1}{\theta}\int \breve{\omega}_\gamma \mathcal{J}^{p,\mathrm{p}}_\gamma d^6\boldsymbol{\xi}\,, \tag{103}$$

with the thermodynamic flux representative of viscoplastic deformation given by

$$\mathcal{J}^{p,\mathrm{p}}_\alpha(\boldsymbol{\xi}) = \int \lambda_{\alpha\gamma}(\boldsymbol{\xi},\boldsymbol{\xi}')\left(\left(\frac{1}{T}-\frac{1}{\theta}\right)\breve{\omega}_\gamma(\boldsymbol{\xi}') - \frac{1}{T}\nabla^{Q'}_\gamma\left[\frac{\delta U_{\mathrm{p}}}{\delta p'} - T\frac{\delta S_{\mathrm{p}}}{\delta p'}\right]\right) d^6\boldsymbol{\xi}'\,, \tag{104}$$

and the abbreviation

$$\breve{\omega}_\gamma = \omega_\gamma + (1-\varphi)\,\nabla^Q_\gamma\left(\frac{\delta U_{\mathrm{p}}}{\delta p} - T\frac{\delta S_{\mathrm{p}}}{\delta p}\right). \tag{105}$$

It should be noted that at thermal equilibrium, $\theta = T$, and for $\breve{\omega}_\gamma = 0$, the evolution equation (102) for T is the same as the temperature equation in the earlier two-scale model [5], where aging and mechanical rejuvenation has not been considered.

A physically meaningful choice for $\breve{\omega}_\alpha$ can be made by considering the consequences of mechanical rejuvenation in more detail [35]. For the modeling of the mechanical rejuvenation of bulk polymer glasses, it has been suggested that mechanical rejuvenation leads to an increase of the configurational temperature [15,16]. Transferring this to the case of glassy bridges modeling in this paper, implies that the last term on the right-hand side of (103) must be positive semi-definite always. This can be achieved by specifying $\breve{\omega}_\alpha$ in such a way that the product $\breve{\omega}_\alpha \mathcal{J}^{p,\mathrm{p}}_\alpha$ is a quadratic form, specifically by

$$\breve{\omega}_\gamma = \frac{\mathfrak{T}}{T + \mathfrak{T}(1-\frac{T}{\theta})}\,\nabla^Q_\gamma\left(\frac{\delta U_{\mathrm{p}}}{\delta p} - T\frac{\delta S_{\mathrm{p}}}{\delta p}\right), \tag{106}$$

with a positive prefactor $\mathfrak{T}$. For simplicity, we choose $\mathfrak{T} = \theta$, which in turn simplifies the thermodynamic flux as well as the evolution equations significantly.

4.2 Specification of energy E and entropy S, and dissipative matrix $\boldsymbol{\lambda}$

For filler-particle contribution to the energy and entropy, we use the assumptions (25)–(30) made in Sec. 3.2, specifically (see also [5])

$$U_{\rm p}[p] = \iint p\,\Phi^{\rm E} d^6\boldsymbol{\xi} d^3\boldsymbol{r}\,, \tag{107}$$

$$S_{\rm p}[p] = -\iint p\left(\frac{\Phi^{\rm S}}{T} + k_{\rm B}\ln p\right) d^6\boldsymbol{\xi} d^3\boldsymbol{r}\,. \tag{108}$$

These expressions imply

$$\nabla^Q_\gamma\left(\frac{\delta U_{\rm p}}{\delta p} - T\frac{\delta S_{\rm p}}{\delta p}\right) = \nabla^Q_\gamma\Phi + k_{\rm B}T\frac{\nabla^Q_\gamma p}{p}\,, \tag{109}$$

which enters at several spots in the complete dynamic model, most prominently in the stress tensor (94) and the viscoplastic deformation of the glassy bridges (104). The first term on the r.h.s. of (109) is a deterministic force, while the second term is a statistical contribution.

In the remainder of this paper, a Hookean spring potential is used for the energy $\Phi(\boldsymbol{\xi})$ associated with the mismatch between the current ($\boldsymbol{R}$) and the load-free ($\boldsymbol{Q}$) state [5],

$$\Phi(\boldsymbol{\xi}) = \Phi^{\rm E}(\boldsymbol{\xi}) + \Phi^{\rm S}(\boldsymbol{\xi}) = \frac{1}{2}k(\boldsymbol{R}-\boldsymbol{Q})^2\,, \tag{110}$$

with spring constant k. In this case, $\nabla^Q_\gamma\Phi = k(Q_\gamma - R_\gamma)$. Therefore, with the aid of (109), one concludes that the deterministic contributions to both the filler-particle related contribution to the stress tensor (94) as well as to the viscoplastic deformation (104) vanish as the current state $\boldsymbol{R}$ becomes equal to the load-free state $\boldsymbol{Q}$, as expected. This leaves only the statistical contributions, related to the second term on the r.h.s. of (109), in the stress tensor and the viscoplastic deformation.

The elastomer-matrix contribution to the energy and entropy,

$$U_{\rm em} = \int u_{\rm em}(T,\theta,\boldsymbol{F}) d^3\boldsymbol{r}\,, \tag{111}$$

$$S_{\rm em} = \int s_{\rm em}(T,\theta,\boldsymbol{F}) d^3\boldsymbol{r}\,, \tag{112}$$

can be derived from the Helmholtz free energy $a_{\rm em}$ by way of

$$u_{\rm em} = a_{\rm em} - T\frac{\partial a_{\rm em}}{\partial T}\,, \quad s_{\rm em} = -\frac{\partial a_{\rm em}}{\partial T}\,. \tag{113}$$

As a slight extension of [5] with respect to a dependence on the configurational temperature θ, we use for illustration purposes

$$a_{\rm em} = \frac{G_{\rm em}(T)}{2}(J_1 - 3 - 2\ln J) + \frac{\kappa_{\rm em}(T)}{2}(\ln J)^2 + \rho\, a_\theta(\theta)\,, \tag{114}$$

where $G_{\rm em}$ and $\kappa_{\rm em}$ denote the T-dependent shear and bulk moduli, respectively, $J_1 = {\rm tr}(\boldsymbol{F}^\top\cdot\boldsymbol{F})$, and $J = \det\boldsymbol{F}$. It should be noted that the only θ-dependent contribution is the last one on the r.h.s. of (114).

To specify the viscoplastic deformation of the glassy bridges, the dissipative matrix $\lambda_{\alpha\beta}$ in (104) needs to be specified. In complete analogy to [5], the following form is adopted,

$$\lambda_{\alpha\beta}(\boldsymbol{\xi},\boldsymbol{\xi}') = \delta(\boldsymbol{R}-\boldsymbol{R}')\delta(\boldsymbol{Q}-\boldsymbol{Q}')\frac{\theta p}{\zeta}\delta_{\alpha\beta}\,, \tag{115}$$

with a friction coefficient ζ, with $\zeta > 0$. The ansatz (115) implies that there is no inherent material anisotropy, and the viscoplastic flux $\mathcal{J}^{p,{\rm p}}_\alpha(\boldsymbol{\xi})$ depends on the driving force only for $\boldsymbol{\xi}' = \boldsymbol{\xi}$.

4.3 Resulting simplified model

Compilation of all of the model specifications discussed in Sec. 4.1 and Sec. 4.2, and further assuming that one is interested in situations of constant kinetic temperature, $D_t T = 0$, the model reduces to

$$D_t\theta = -\frac{1}{\tau_{\mathrm{R}}}(\theta - T) + \frac{1}{\theta\eta_{,\theta}}\int \frac{p}{k\tau_\alpha}\left(k(Q_\gamma - R_\gamma) + k_{\mathrm{B}}T\frac{\nabla^Q_\gamma p}{p}\right)^2 d^6\boldsymbol{\xi}\,, \tag{116}$$

$$\begin{aligned}\partial_t p = {} & -\nabla^r_\gamma\left(p v_\gamma\right) - \nabla^R_\gamma\left(\left[\nabla^r_\mu v_\gamma\right]^{\mathrm{sym}} R_\mu p\right) \\ & -\nabla^Q_\gamma\left[\left(-\frac{1}{\tau_\alpha}(Q_\gamma - R_\gamma) + \frac{k_{\mathrm{B}}T}{k}\left(\nabla^Q_\gamma\frac{1}{\tau_\alpha}\right)\right)p\right] + \nabla^Q_\gamma\nabla^Q_\gamma\left(\frac{k_{\mathrm{B}}T}{k\tau_\alpha}p\right)\,,\end{aligned} \tag{117}$$

together with the evolution of the deformation gradient (92) and the momentum balance (89). With the ansatz (114), the Cauchy stress tensor (94) takes the specific form

$$\sigma_{\alpha\gamma} = (a_{\mathrm{em}} + \kappa_{\mathrm{em}}\ln J - 2nk_{\mathrm{B}}T)\,\delta_{\alpha\gamma} + G_{\mathrm{em}}\,(B_{\alpha\gamma} - \delta_{\alpha\gamma}) + \int p\left[R_\gamma\big(\nabla^R_\alpha\Phi\big)\right]^{\mathrm{sym}}\mathrm{d}^6\boldsymbol{\xi}\,, \tag{118}$$

with $n = \int p d^6\boldsymbol{\xi}$ the number density of representative pairs, and the left Cauchy-Green strain tensor $B_{\alpha\gamma} = F_{\alpha\mu}F_{\gamma\mu}$. To obtain (118), the relations (95), (96), and (107)–(109) have been employed. In the above, it has been used that, by virtue of the ansatz (114), the configurational entropy density per unit mass, η/ρ with $\eta = -\partial a_{\mathrm{em}}/\partial\theta|_{\boldsymbol{F},T} = -\rho(\mathrm{d}a_\theta/\mathrm{d}\theta)$, is independent of $\boldsymbol{F}$, which eventually results in the absence of $(\nabla^r_\mu v_\gamma)$-related contributions to (116). Furthermore, two relaxation times have been defined, namely the time scale τ_{R} for the relaxation of the configurational temperature θ towards T, and the time scale τ_α for the relaxation of the load-free state $\boldsymbol{Q}$ towards $\boldsymbol{R}$,

$$\tau_{\mathrm{R}} = \frac{T\theta^2\eta_{,\theta}}{\mu^{\mathrm{x}}}\,, \tag{119}$$

$$\tau_\alpha = \frac{\zeta}{k}\,. \tag{120}$$

In all equations, the friction coefficient ζ is eliminated in favor of τ_α, and μ^{x} in favor of τ_{R}.

For computational purposes, it is convenient to realize that the above Fokker-Planck equation (117) can be translated into an equivalent system of stochastic differential equations [41], specifically

$$\mathrm{d}R_\gamma = \left[\nabla^r_\mu v_\gamma\right]^{\mathrm{sym}} R_\mu \mathrm{d}t\,, \tag{121}$$

$$\mathrm{d}Q_\gamma = -\frac{1}{\tau_\alpha}(Q_\gamma - R_\gamma)\mathrm{d}t + \frac{k_{\mathrm{B}}T}{k}\left(\nabla^Q_\gamma\frac{1}{\tau_\alpha}\right)\mathrm{d}t + \sqrt{\frac{2k_{\mathrm{B}}T}{k\tau_\alpha}}\mathrm{d}W_{\mathrm{t}\gamma}\,, \tag{122}$$

which will be used for the numerical simulations in Sec. 5. The last term in (122) represents the fluctuating Brownian contributions, that add stochasticity to the $\boldsymbol{Q}$-dynamics. The symbol $\mathrm{d}\mathbf{W}_t$ stands for increments of Wiener processes [41], with average and variance

$$\langle \mathrm{d}\,W_{t\alpha}\rangle = 0\,, \tag{123}$$

$$\langle \mathrm{d}\,W_{t\alpha}\mathrm{d}W_{t'\beta}\rangle = \delta_{\alpha\beta}\,\delta_{tt'}\,\mathrm{d}t\,, \tag{124}$$

respectively. In other words $\mathrm{d}\mathbf{W}_t$ represents white noise, being uncorrelated in time. It is pointed out that the stochastic differential equations (122) are to be interpreted in the Itô-sense [41], which is convenient for an explicit forward Euler integration of the system of equations (121) and (122) in Sec. 5.

4.4 Relaxation processes

In the system of evolution equations presented in Sec. 4.3, the relaxation times τ_{R} and τ_α require further specification, which is discussed in this section.

The relaxation time τ_α for the vector $\boldsymbol{Q}$ contains all the information about temperature- and load-dependence of the thermo-mechanics of the glassy bridges. To specify this dependence, the procedures outlined in [8–10] are followed, as done in our earlier work [5], and the reader is referred to those publications for further detail. At this point, the main physical features encoded in τ_α are briefly

summarized. If the elastomer matrix material adheres well to the particle surface, the mobility of the elastomer chain segments decreases as the filler-particle surface is approached, which can be captured phenomenologically by an increase in the local glass-transition temperature. At a certain distance this increase is such that even at room temperature there exists a glassy layer around the particles. Formally, the shift of glass transition temperature due to the fillers can be described by $T_{\mathrm{g}}(z) = T_{\mathrm{g,b}}(1 + \beta/z)$, where $T_{\mathrm{g,b}}$ stands for bulk glass transition temperature, β accounts for the strength of the particle-matrix interaction, and z is the distance from the particle surface [3,4]. On the other hand, an applied dynamic load increases the mobility of matrix material around filler particles, i.e., effectively resulting in a decrease of the local glass transition temperature. Considering two particles with a local interparticle mechanical load Σ_{loc} and separated by a surface-to-surface distance $|\boldsymbol{R}| - d = 2z$ with filler-particle diameter d, the glass transition temperature relevant for that respective glassy bridge is given by [8,9]

$$T_{\mathrm{g}}(z, \Sigma_{\mathrm{loc}}) = T_{\mathrm{g,b}} \left(1 + \frac{\beta}{z}\right) - \frac{\Sigma_{\mathrm{loc}}}{K}\,, \tag{125}$$

where K relates the yield stress σ_{y} to the glass transition temperature T_{g} by way of the relation $\sigma_{\mathrm{y}} = K(T_{\mathrm{g}} - T)$. Both K and β are material parameters that can be experimentally measured.

In [5,8,9], a relation between the relaxation time τ_α and the local glass transition temperature (125) has been employed. In this paper, this relation is extended in order to account for the configurational temperature θ, i.e., to account for the effects of physical aging and mechanical rejuvenation. This is achieved by employing the Hodge-Scherer equation [42–44]

$$\tau_\alpha \quad = \quad \tau_{\mathrm{g}} \exp\left[-c_1 \frac{c_2(T-\theta) + T(\theta - T_g(z, \Sigma_{\mathrm{loc}}))}{T(c_2 + \theta - T_g(z, \Sigma_{\mathrm{loc}}))}\right]\,, \tag{126}$$

with c_1 and c_2 the polymer-specific WLF parameters, and τ_{g} the relaxation time at $T = \theta = T_{\mathrm{g}}$. It should be noted that the expression above for the relaxation time τ_α converges to the conventional WLF law [45] at $\theta = T$, in other words for a completely aged sample the relaxation time is governed by the usual WLF law. As explained in [5], the scalar measure Σ_{loc} for the local interparticle stress can be approximated by

$$\Sigma_{\mathrm{loc}} \quad = \quad \sqrt{|I_2|}\,, \tag{127}$$

where I_2 is the second invariant, namely $I_2 = (1/2)[(\mathrm{tr}\boldsymbol{\Sigma})^2 - \mathrm{tr}(\boldsymbol{\Sigma} \cdot \boldsymbol{\Sigma})]$, of the local interparticle stress tensor

$$\boldsymbol{\Sigma}_{\mathrm{loc}} = \left[\boldsymbol{R}\nabla^R \Phi_{\mathrm{t}}\right]\,. \tag{128}$$

For completeness, it is mentioned that Φ_{t} in (128) does not only contain the glassy-bridge contribution specified in (110), but also a second contribution that represents the elastomer matrix stress on the particle level; the reader is referred to Sec. 4.2 in [5] for further details.

As far as the specification of the relaxation time τ_{R} is concerned, i.e., the approach of the configurational (θ) to the kinetic (T) temperature during physical aging, we refer to [44]. In particular, there it was argued that τ_{R} shares the same type of relaxation as that specified for τ_α in (126), with the only exception that the local interparticle load is not included. Therefore,

$$\tau_{\mathrm{R}} \quad = \quad \tau_{\mathrm{R}}^0 \exp\left[-c_1 \frac{c_2(T-\theta) + T(\theta - T_g(z, 0))}{T(c_2 + \theta - T_g(z, 0))}\right]\,, \tag{129}$$

with τ_{R}^0 a constant, positive prefactor.

5 Numerical solution

5.1 Coupling of micro-scale to macro-scale components

The numerical solution of the model summarized in Sec 4.3 is cumbersome. On the one hand, there is an influence of the macroscopic state of the system, e.g. through the temperature T and the imposed velocity field $\boldsymbol{v}$ on the microscopic dynamics (117), or (121)–(122), respectively. On the other hand, the microscopic state enters the evolution of the configurational temperature of the elastomer θ on the

macroscopic scale by way of the second term on the r.h.s. of (116). This is exactly the source of complications when attempting to solve this coupled system of equations numerically, as explained in the following.

As mentioned earlier, it is convenient to solve the configurational temperature evolution (116) in combination with the stochastic differential equations (121)–(122), rather than in combination with the Fokker-Planck equation (117). Specifically, (121) is an ordinary differential equation, which in many cases might be solved analytically, to determine the motion of vector $\boldsymbol{R}$ due to the imposed deformation. The vector $\boldsymbol{Q}$, that stands for a load-free particle configuration, is described by the stochastic differential equation (122). Inspecting the structure of both of these evolution equations together with the fact that the Itô-calculus applies for their stochastic interpretation [41], as mentioned in Sec. 4.3, one concludes that conventional numerical techniques can be employed for solving (121)–(122) (see e.g. [41]). The situation, however, looks more involved if one attempts to solve (121)–(122) simultaneously with (116), for the following reason. The integral on the r.h.s. of (116) can be expressed as a series of terms in powers of $k_{\mathrm{B}}T$, namely

$$I = \int \frac{p}{k\tau_\alpha} \left(k(Q_\gamma - R_\gamma) + k_{\mathrm{B}}T \frac{\nabla^Q_\gamma p}{p} \right)^2 d^6\boldsymbol{\xi} = I_1 + I_2 + I_3 \geq 0\,, \tag{130}$$

with the definitions

$$I_1 = k \int \frac{1}{\tau_\alpha} \left(R_\gamma - Q_\gamma\right)^2 p\, d^6\boldsymbol{\xi}\,, \tag{131}$$

$$I_2 = 2k_{\mathrm{B}}T \int \left[(R_\gamma - Q_\gamma) \left(\nabla^Q_\gamma \frac{1}{\tau_\alpha} \right) - \frac{3}{\tau_\alpha} \right] p\, d^6\boldsymbol{\xi}\,, \tag{132}$$

$$I_3 = -\frac{(k_{\mathrm{B}}T)^2}{k} \int \left[\nabla^Q \left(\frac{1}{\tau_\alpha} \nabla^Q \ln p \right) \right] p\, d^6\boldsymbol{\xi}\,. \tag{133}$$

In the first two integrals, I_1 and I_2, the function p as such occurs as a multiplicative factor in the integral. Denoting the respective integrand divided by p as as i_k, i.e. $I_k = \int i_k\, p\, d^6\boldsymbol{\xi}$ for $k = 1, 2$, these integrals can be interpreted in terms of averages of i_k with respect to the microscopic filler-particle arrangement. From a simulation perspective, this means that one could simulate a large number of realizations of $\boldsymbol{R}$- and $\boldsymbol{Q}$-dynamics, measure for each of the realizations the quantity i_k, and then averaging that over all realizations. This is exactly the procedure used in the CONNFFESSIT (Calculation of Non-Newtonian Flow: Finite Elements and Stochastic Simulation Techniques) approach [41, 46]. However, inspection of (133) makes clear that such a procedure can not be applied to I_3, because in this case one obtains $i_3 = -(k_{\mathrm{B}}^2T^2/k)\nabla^Q \left(\tau_\alpha^{-1}\, \nabla^Q \ln p\right)$, which can not be measured for each realization individually but rather depends on the distribution of all realizations. Therefore, the possibilities are to either search for a new technique that can deal with the type of coupling represented in I_3 or, alternatively, one tries to assess how significant the contribution I_3 to the entire integral I actually is.

5.2 Gaussian approximation

As it was mentioned in the previous section, the CONNFFESSIT approach can in general not be applied to the model developed in this paper due to the specific form of the contribution I_3, given in (133). However, one can attempt to estimate the relative magnitude of the three contributions (131)–(133) to the total integral I (130), under certain circumstances, which is the purpose of this section.

The specific case, for which a concrete calculation of the three contributions to (130) can be performed is when the relaxation time τ_α does not depend on $\boldsymbol{Q}$ (and $\boldsymbol{R}$). In this case, the distribution corresponding to the Fokker-Planck equation (117), or the corresponding stochastic differential equations (121)–(122), respectively, is Gaussian [41]. Specifically, the Gaussian distribution can be written in the form

$$p(\boldsymbol{r}, \boldsymbol{\xi}) = N \exp\left\{ -\frac{1}{2}\, \xi_\alpha\, \Theta^{-1}_{\alpha\beta}\, \xi_\beta \right\}\,, \tag{134}$$

with normalization constant $N = (2\pi)^{-3}(\det \boldsymbol{\Theta})^{-1/2}$, and the symmetric positive semi-definite matrix $\boldsymbol{\Theta}$, defined by

$$\boldsymbol{\Theta} = \left\langle \boldsymbol{\xi}\, \boldsymbol{\xi} \right\rangle = \begin{pmatrix} \langle \boldsymbol{R}\, \boldsymbol{R} \rangle & \langle \boldsymbol{R}\, \boldsymbol{Q} \rangle \\ \langle \boldsymbol{Q}\, \boldsymbol{R} \rangle & \langle \boldsymbol{Q}\, \boldsymbol{Q} \rangle \end{pmatrix}\,, \quad \text{with} \quad \langle \boldsymbol{R}\, \boldsymbol{Q} \rangle = \langle \boldsymbol{Q}\, \boldsymbol{R} \rangle^\top\,. \tag{135}$$

After straight-forward calculation one can show that

$$\nabla_\alpha^Q \ln p \;=\; \lambda_{\alpha\varepsilon}\Big(\mu_{\varepsilon\gamma} R_\gamma - Q_\varepsilon\Big)\,, \tag{136}$$

with

$$\lambda_{\alpha\varepsilon} \;\equiv\; \Big[\langle \boldsymbol{Q}\,\boldsymbol{Q}\rangle - \langle \boldsymbol{Q}\,\boldsymbol{R}\rangle \cdot \langle \boldsymbol{R}\,\boldsymbol{R}\rangle^{-1} \cdot \langle \boldsymbol{R}\,\boldsymbol{Q}\rangle\Big]^{-1}_{\alpha\varepsilon}\,, \tag{137}$$

$$\mu_{\varepsilon\gamma} \;\equiv\; \big[\langle \boldsymbol{Q}\,\boldsymbol{R}\rangle \cdot \langle \boldsymbol{R}\,\boldsymbol{R}\rangle^{-1}\big]_{\varepsilon\gamma}\,. \tag{138}$$

With the representation (136), all integrals I_k specified in (131)–(133) can be expressed in terms of the second moments (135),

$$I_1 \;=\; \frac{k}{\tau_\alpha}\Big(\langle R_\gamma R_\gamma\rangle - 2\langle R_\gamma Q_\gamma\rangle + \langle Q_\gamma Q_\gamma\rangle\Big)\,, \tag{139}$$

$$I_2 \;=\; -\frac{6k_{\mathrm{B}}T}{\tau_\alpha}\,, \tag{140}$$

$$I_3 \;=\; \frac{k_{\mathrm{B}}^2T^2}{k\tau_\alpha}\lambda_{\gamma\gamma}\,, \tag{141}$$

where $\lambda_{\alpha\varepsilon}$ is given by (137).

For the simulations performed in Sec. 5.4, the relative importance of the three contributions will be examined, with the goal to identify those conditions under which I_3 can be neglected, and thus the CONNFFESSIT approach could be employed for solving the dynamics of the model specified in Sec. 4.3 and Sec. 4.4.

5.3 Simulation setup and model parameters

Table 1: Parameters of the model. The values of the parameters correspond to particle volume fraction $\phi = 0.4$.

parameter	symbol	physical value
particle diameter	d	$2 \cdot 10^{-8}$ m
number density of pairs	n	$1.05 \cdot 10^{23}$ m^{-3}
bulk glass transition temperature	$T_{\mathrm{g,b}}$	213 K
relaxation time	τ_{g}	100 s
relaxation time of heat exchange	τ_{R}^0	0.74 s
temperature of the experiment	T	263 K
distance-sensitivity parameter	β	$9 \cdot 10^{-10}$ m
stress-sensitivity parameter	K	$2 \cdot 10^{-20}$ J K^{-1}
glassy spring constant	k	1.94 N/m
elastomer spring constant	k_{em}	$k/50$ (see [10])
WLF-constants	C_1, C_2	12.8, 34 K
shear modulus elastomer	G_{em}	10^6 Pa
heat capacity of configurational subsystem of elastomer matrix	$c_\theta = \theta\eta_{,\theta}$	$2.5 \cdot 10^5$ J m^{-3}

In Sec. 4, we have made assumptions on the energy and entropy, as well as on the dynamics of the glassy bridges and the heat exchange between the two thermal subsystems of the elastomer matrix. To solve the model presented in Sec. 4.3 and Sec. 4.4 numerically, the CONNFFESSIT approach [41] is used, in order to obtain the stress-strain response for isothermal conditions, i.e. $D_tT = 0$, with physical aging and mechanical rejuvenation. The CONNFFESSIT approach is chosen in anticipation of the outcome that (see Sec. 5.4), for the conditions studied numerically in this paper, I_3 defined in (133) can be neglected in comparison to the other contributions to (130).

The particle configuration used for the initial state is the same as was used in our earlier publication [5], specifically the initial configuration corresponds to the unloaded state, $\boldsymbol{R} = \boldsymbol{Q}$. In addition,

the vector $\boldsymbol{R}$ is isotropically distributed, i.e. the length $R = |\boldsymbol{R}|$ was sampled from a narrow distribution of the form $w(R) \propto (d - \langle R \rangle)^2 - (R - \langle R \rangle)^2$ for $R \in [d, 2\langle R \rangle - d]$. This distribution has mean $\langle R \rangle = d/\sqrt[3]{\phi} = 2.71 \cdot 10^{-8}$m and standard deviation $\sqrt{\langle R^2 \rangle - \langle R \rangle^2} = (\langle R \rangle - d)/\sqrt{5} = 3.2 \cdot 10^{-9}$m for volume fraction $\phi = 0.4$. To this initial particle configuration, an oscillatory shear deformation is applied with a velocity field of the form $\boldsymbol{v} = (v_1, v_2, v_3)$ with components $v_1(r_2, t) = \dot{\gamma}(t) r_2$ and $v_2 \equiv v_3 \equiv 0$. The time-dependent imposed deformation is sinusoidal,

$$\gamma(t) = \gamma_0 \sin(\omega t), \tag{142}$$

with amplitude γ_0 and angular frequency ω.

The parameters used for the numerical study are listed in Table 1, and are closely related to those considered in [5] for particle volume fraction $\phi = 0.4$. The matrix material, in which the silica nanoparticles are uniformly dispersed, is a poly(ethyl acrylate) matrix. All these parameters can be related to physical parameters, as explained in [8]. In particular, the value we chose for the parameter $\beta = 0.9$ nm, which sets the amplitude of the T_{g}-shift in the vicinity of the filler particles, corresponds to that measured experimentally in [3, 4]. In the simulations, the stress-induced shift in the glass transition temperature (125) has been limited to ≤ 200 K, since above that value the system is already plasticized (see also [9]). For numerical reasons, the range of the relaxation time (126) has been limited to $0.01 \text{ s} \leq \tau_\alpha \leq 100 \text{ s}$ [10]. For the simulation presented below, the initial relaxation time is equal to $\langle \tau_\alpha^{\mathrm{init}} \rangle = \tau_{\mathrm{g}}$.

The specific choice for the heat capacity of the configurational subsystem of the elastomer matrix $c_\theta = \theta \eta_{,\theta}$ needs to be explained, since this is an aspect of the model that was absent in [5]. To determine its value, we have taken the corresponding value, i.e. the heat capacity per unit mass $\Delta c = 0.25 \text{ Jg}^{-1}\text{K}^{-1}$, used in [16]. In contrast, in this paper, η is expressed per unit volume of the entire nanocomposite, and therefore $c_\theta = \rho_{\mathrm{g}} \Delta c$, with ρ_{g} the mass density of glassy network per unit volume of the entire nanocomposite. One can show that $\rho_{\mathrm{g}} = \rho_{\mathrm{em}} \phi [(1 + 2\delta/d)^3 - 1]$, where ρ_{em} represents the mass density of elastomer matrix per unit volume of elastomer matrix, and δ is the thickness of the glassy layer around the filler particle, that depends of temperature and particle-matrix interaction. The value for c_θ, listed in Table 1 corresponds to $\phi = 0.4$, $d = 2 \cdot 10^{-8}$m, $\delta = 3.834 \cdot 10^{-9}$m and $\rho_{\mathrm{em}} = 1.52 \cdot 10^6 \text{g m}^{-3}$.

5.4 Assessment of the Gaussian approximation

Simulations have been performed in order to judge the relative importance of the three contributions to the integral (130), which stands for the effect of mechanical rejuvenation on the configurational temperature, see (116). To that end, simulations have been performed, using the above specifications and for $\theta = T$. Three simulations have been conducted under oscillatory shear deformation with deformation amplitudes $\gamma_0 = 0.1$, $\gamma_0 = 0.2$, and $\gamma_0 = 0.3$. For each deformation amplitude, an intermediate frequency has been chosen such that the material response shows both elastic as well as viscoplastic contributions. At $\gamma_0 = 0.1$, one finds $|I_1/I_2| > 20$ and $|I_2/I_3| \simeq 11$. When increasing the amplitude to $\gamma_0 = 0.2$, $|I_1/I_2| > 65$ and $|I_2/I_3| \simeq 25$. Finally, at the largest deformation amplitude $\gamma_0 = 0.3$, $|I_1/I_2| > 63$ and $|I_2/I_3| \simeq 40$. The conclusion is that, under the conditions studied, the Gaussian approximation predicts $I_1 > I_2 > I_3$, with factors of order ten or more in between. This suggests that one might neglect the I_3-contribution to I. It should be emphasized, however, that this conclusion can only hold if the deformation is sufficiently strong. Or, conversely, at equilibrium I_3 must be of similar order of magnitude like the other terms. This originates from the fact that the term in parenthesis in (130) vanishes for the equilibrium distribution, according to (117). Therefore, $I = 0$ at equilibrium implies that I can not be dominated simply by I_1, but rather that also I_2 and I_3 contribute significantly.

According to the Gaussian approximation, one may thus neglect the third contribution I_3 to the integral (130) when performing simulations at strong enough deformation. In the following section, simulations are performed for $\gamma_0 = 0.3$, for which the third integral I_3 is much smaller than the other two if the Gaussian approximation is used. To what extent this implies that the third contribution I_3 can be neglected also in the absence of the Gaussian approximation, i.e. when performing CONNFFESSIT-type simulations, this is discussed below.

5.5 Simulation of physical aging in filled elastomers

The main goal of this section is to study the dynamic model described in Sec. 4.3 and Sec. 4.4 numerically, in order to assess how the mechanical response of the entire nanocomposite is affected by physical aging

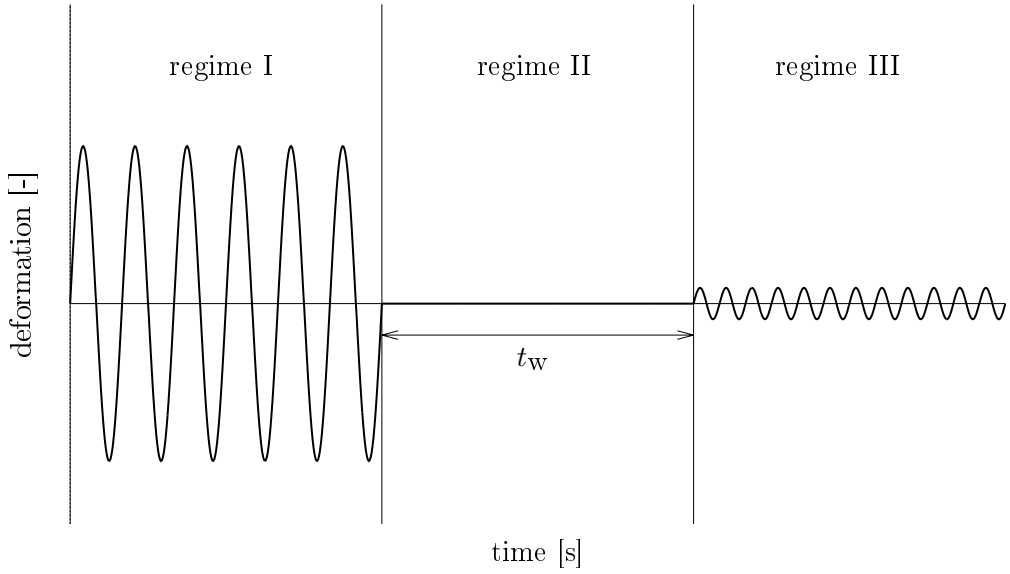

Figure 1: Deformation protocol: To an initially aged sample, large amplitude oscillatory deformation is applied (region I), followed by a deformation-free period of duration t_{w} (region II). Finally, after the waiting time t_{w}, the mechanics of the sample is probed under small amplitude oscillatory deformation (region III).

and mechanical rejuvenation of the interparticle matrix material, both of these effects being implemented in the configurational temperature evolution (116). The specific deformation protocol employed in this paper has been described in [8, 9] for studying the Mullins effect in a wider context. The deformation protocol contains the following components, also shown in Figure 1. Starting with a state of mechanical equilibrium and with an aged state with $\theta \geq T$, large amplitude oscillatory shear deformation is applied. It is anticipated that this results in the mechanical rejuvenation of the nanocomposite (region I). This is followed by letting the system at rest for a certain waiting period t_{w} (region II). Finally, the linear viscoelastic properties are measured (region III), and the effect of the waiting time t_{w} is studied.

5.5.1 Mechanical rejuvenation (regime I)

Mechanical rejuvenation is represented by the second term on the r.h.s. of the configurational temperature evolution (116), namely in terms of I given by (130). It can thus be anticipated that, upon the application of substantial deformation, the configurational temperature θ will increase with increasing time of deformation, by virtue of $I \geq 0$ (see (130)). More specifically, the rate of change of θ in (116) consists of two contributions with different signs. On the one hand, according to the first term on the r.h.s. of (116), the difference of temperatures always leads to decrease of θ to T, for $\theta \geq T$. On the other hand, according to the second term on the r.h.s. of (116), the deformation always leads to an increase of θ, due to the mechanical rejuvenation, $I \geq 0$. Therefore, there is a competition between physical aging and mechanical rejuvenation. This fact one can use to determine the yet undetermined prefactor τ_{R}^0 in (129), such that under certain loading conditions, θ approaches the local glass transition temperature from below, but does not surpass it as the deformation is continued for a prolonged period of time, i.e. a steady state is reached. By performing several simulations, we have determined the parameter τ_{R}^0 such that the θ asymptotically approaches the statistical average of the initial (in the undeformed configuration) local glass transition temperature, $\langle T_{\mathrm{g}}^{\mathrm{init}}(z,0)\rangle$, for $\gamma_0 = 0.3$ and $\omega = 20\,\mathrm{s}^{-1}$. For this deformation protocol, the corresponding shear stress, the configurational temperature, and the first and second integrals (I_1 and I_2) are shown in Fig. 2.

With respect to these simulations in regime I of Fig. 1, the reader is reminded of the Gaussian approximation considerations in Sec. 5.4 that lead us to conclude that the contribution I_3 to I in (130)

can be neglected, specifically also for the conditions studied above, $\gamma_0 = 0.3$ and $\omega = 20\,\mathrm{s}^{-1}$. In the absence of the Gaussian approximation, the error introduced by neglecting I_3 can not be assessed easily. However, one can instead study the relative importance of the first two contributions, I_1 and I_2, and compare that to the prediction for the Gaussian approximation. This would serve, partly, as an *a posteriori* justification for using the CONNFFESSIT approach. As we can see from Fig. 2(c), even at the early stages of deformation, I_1 dominates over I_2, while as we will see later on, this statement does not hold for smaller deformation rates. When the system goes towards the regime of an oscillatory steady-state, the value of I_1 is significantly larger than I_2. This can be quantified in terms of the time averages of these two integrals, $\langle I_1 \rangle$ and $\langle I_2 \rangle$, and specifically their ratio $\langle I_2 \rangle / \langle I_1 \rangle$ can be used as a measure of the applicability of our numerical approach. In short, the numerical approach gets more trustworthy the smaller the ratio $\langle I_2 \rangle / \langle I_1 \rangle$, while the numerical approach is erroneous if $I_1 + I_2$ is negative, since I in (130) is based on a quadratic form and should thus be positive semi-definite. For the particular case simulated for the mechanical rejuvenation in region I with $\gamma_0 = 0.3$ and $\omega = 20\,\mathrm{s}^{-1}$, one obtains $\langle I_1 \rangle = 4.1 \cdot 10^6 \mathrm{N\ m\ s}^{-1}$ and $\langle I_2 \rangle = 9.7 \cdot 10^4 \mathrm{N\ m\ s}^{-1}$, resulting in $\langle I_2 \rangle / \langle I_1 \rangle = 0.024$, which, in combination with the finding $I_1 + I_2 > 0$, suggests that the CONNFFESSIT approach may be used, because it seems admissible to neglect I_3.

Varying the frequency ω of the applied load, one can also see its influence on the evolution of θ. Specifically, one finds $\langle I_2 \rangle / \langle I_1 \rangle = 0.022$ and $I_1 + I_2 > 0$ for $\omega = 15\,\mathrm{s}^{-1}$ (Fig. 3), and $\langle I_2 \rangle / \langle I_1 \rangle = 0.014$ and $I_1 + I_2 > 0$ for $\omega = 10\,\mathrm{s}^{-1}$ (Fig. 4). However, for the lowest frequency studied, $\omega = 5\,\mathrm{s}^{-1}$ (Fig. 5), one observes that $I_1 + I_2$ becomes temporarily negative, which is inadmissible. This clearly indicates that the CONNFFESSIT approach must not be used under these loading conditions.

From these simulation results, one concludes in general that the configurational temperature of the glassy bridges is increased due to mechanical rejuvenation, as expected. In other words, to some extent, the thermal history is erased. This effect is more significant the stronger the applied deformation.

5.5.2 Aging (regime II)

In order to discuss the physical aging in the undeformed state, one can not employ the CONNFFESSIT approach, because in this regime it is not appropriate to neglect the contribution I_3 to (130), as discussed earlier. Instead, the evolution equations for the configurational temperature (116) and for the filler-particle arrangement (117) are studied in a qualitative manner.

At the beginning of region II, p is in a non-equilibrium state, however, it will relax towards the equilibrium state over a period of the order of τ_α. As this relaxation takes place, the mechanical rejuvenation contribution, i.e. the second contribution on the r.h.s. of (116), continuously decreases in magnitude until it vanishes at thermal equilibrium. Simultaneously, the configurational temperature decays from its value $\theta > T$ at the beginning of region II towards T with increasing waiting time t_w, i.e. $\partial\theta/\partial t_\mathrm{w} < 0$. In view of the concrete form of relaxation time τ_α in (126), one can show that a decrease of θ results in an increase of τ_α. In turn, this implies that τ_α increases with increasing waiting time, i.e. with increasing age, $\partial\tau_\alpha/\partial t_\mathrm{w} > 0$.

5.5.3 Probing the linear response (regime III)

In this regime, the linear response of the material is probed, particularly in terms of the storage modulus G' [47]. Specifically, we are interested in whether the model in this paper shows a recovery of the storage modulus G' with waiting time t_w, at a fixed frequency [8, 9]. Similarly to Sec. 5.5.2, also in this case of linear oscillatory deformation it is not appropriate to use the CONNFFESSIT approach for a numerical study of this effect, and therefore we resort to a discussion of the qualitative aspects of the two-scale model.

As discussed in Sec. 5.5.2, the relaxation time τ_α increases with increasing waiting time t_w, and a similar statement also holds for the relaxation time τ_R. This can be used in an argument about the recovery of G' as follows. In general, the storage modulus is an increasing function of frequency. If one assumes for illustration purposes that the storage modulus depends just on a single relaxation time, denoted by τ in the sequel, the storage modulus can be written in the form $G'(\omega, \tau) = G'_0 f(\omega\tau)$ with $\mathrm{d}f(x)/\mathrm{d}x > 0$ and $G'_0 > 0$. One then finds

$$\mathrm{sign}\left(\left.\frac{\partial G'}{\partial t_\mathrm{w}}\right|_\omega\right) = \mathrm{sign}\left(\left.\frac{\partial G'}{\partial \tau}\right|_\omega\right) = \mathrm{sign}\left(\frac{\partial G'}{\partial(\omega\tau)}\right) = \mathrm{sign}\left(\frac{\mathrm{d}f}{\mathrm{d}x}\right) = 1\,, \tag{143}$$

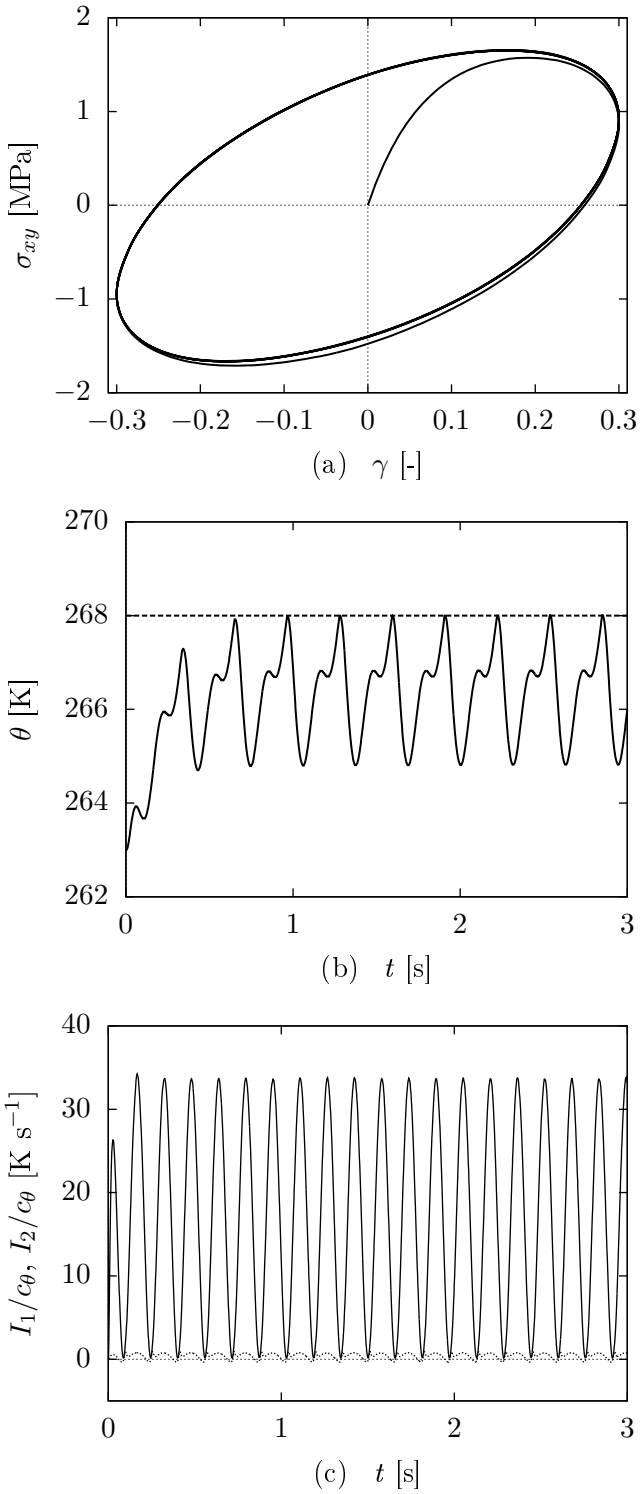

Figure 2: Oscillatory deformation for ten cycles, for deformation amplitude $\gamma_0 = 0.3$ and frequency $\omega = 20\,\mathrm{s}^{-1}$. Shear stress σ_{xy} as a function of the applied shear strain (a). Configurational temperature θ (b), and the quantities I_1/c_θ and I_2/c_θ (see (131) and (132)) (c), as functions of time. The dashed line in (b) denotes the statistical average of the initial local glass transition temperature, $\langle T_{\mathrm{g}}^{\mathrm{init}}(z,0)\rangle$.

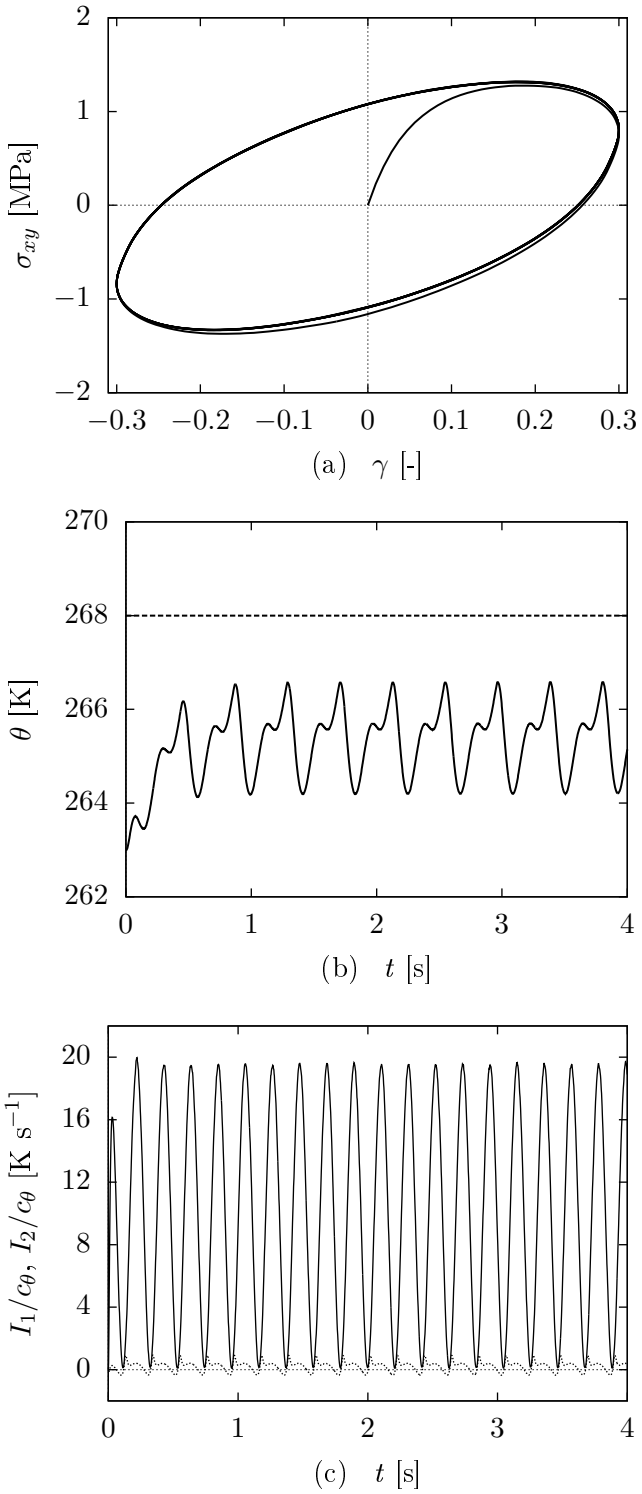

Figure 3: Oscillatory deformation for ten cycles, for deformation amplitude $\gamma_0 = 0.3$ and frequency $\omega = 15\,\mathrm{s}^{-1}$. Shear stress σ_{xy} as a function of the applied shear strain (a). Configurational temperature θ (b), and the quantities I_1/c_θ and I_2/c_θ (see (131) and (132)) (c), as functions of time. The dashed line in (b) denotes the statistical average of the initial local glass transition temperature, $\langle T_{\mathrm{g}}^{\mathrm{init}}(z,0)\rangle$.

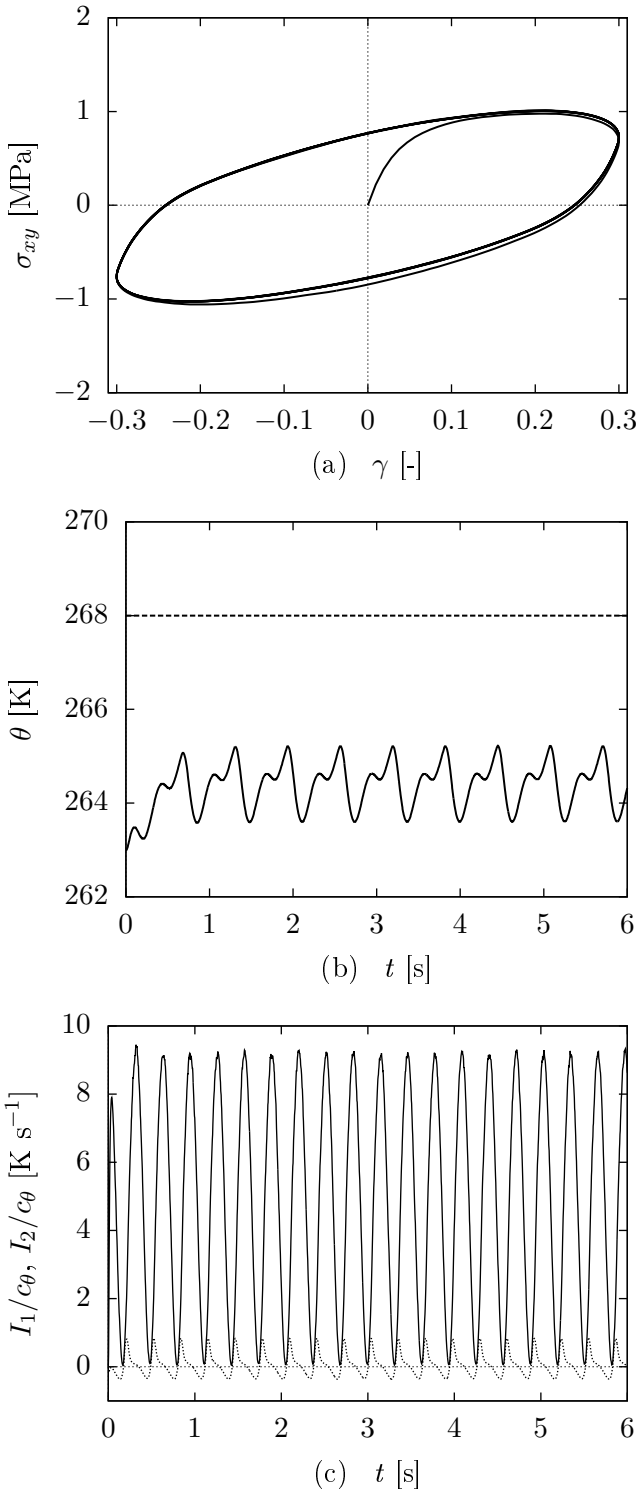

Figure 4: Oscillatory deformation for ten cycles, for deformation amplitude $\gamma_0 = 0.3$ and frequency $\omega = 10\,\mathrm{s}^{-1}$. Shear stress σ_{xy} as a function of the applied shear strain (a). Configurational temperature θ (b), and the quantities I_1/c_θ and I_2/c_θ (see (131) and (132)) (c), as functions of time. The dashed line in (b) denotes the statistical average of the initial local glass transition temperature, $\langle T_{\mathrm{g}}^{\mathrm{init}}(z,0)\rangle$.

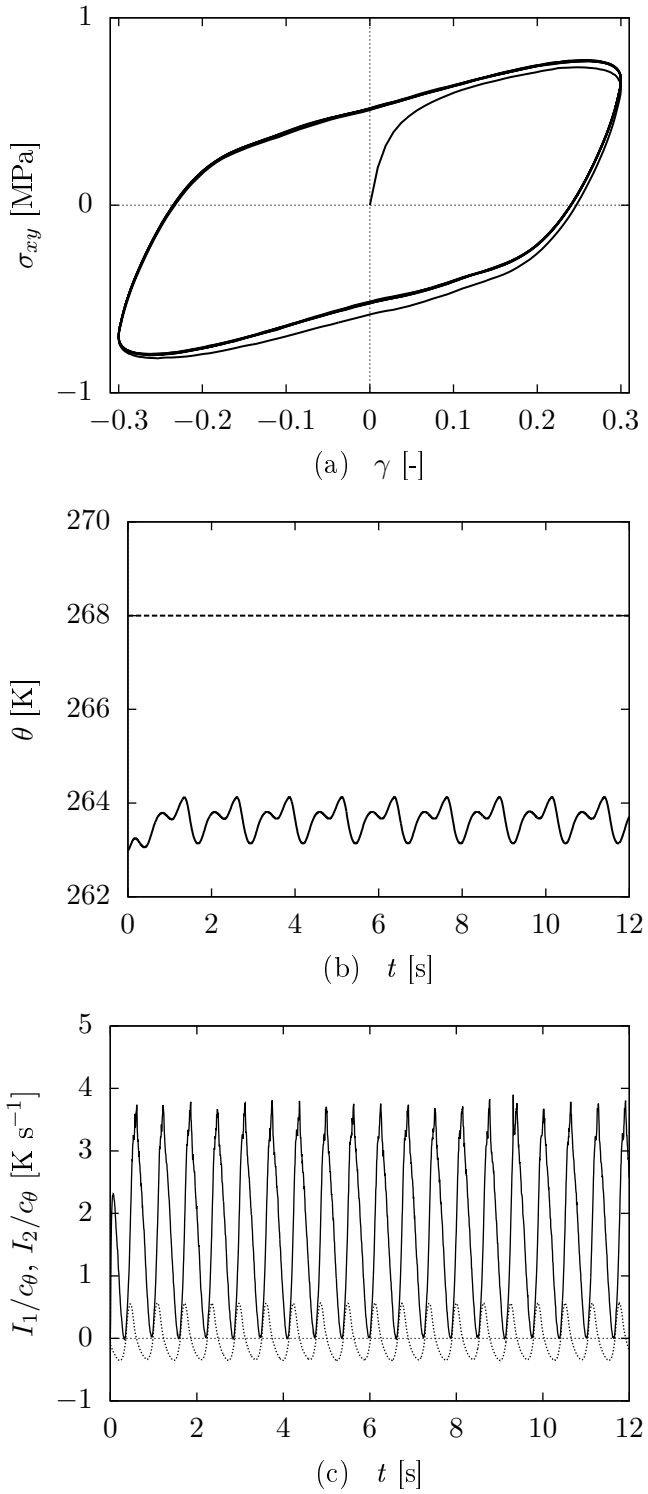

Figure 5: Oscillatory deformation for ten cycles, for deformation amplitude $\gamma_0 = 0.3$ and frequency $\omega = 5\,\mathrm{s}^{-1}$. Shear stress σ_{xy} as a function of the applied shear strain (a). Configurational temperature θ (b), and the quantities I_1/c_θ and I_2/c_θ (see (131) and (132)) (c), as functions of time. The dashed line in (b) denotes the statistical average of the initial local glass transition temperature, $\langle T_{\mathrm{g}}^{\mathrm{init}}(z,0)\rangle$.

where in the first equality we have used $\partial\tau/\partial t_{\mathrm{w}} > 0$. Therefore, one has proven that the storage modulus G' at a fixed frequency increases with waiting time t_{w}, i.e., as the systems ages physically.

In summary, it can be said that the model presented in this paper carries the features necessary for describing the recovery of the elastic modulus G' after large-amplitude oscillatory deformation for hard-particle filled elastomer nanocomposites, according to the protocol described in [8,9]. However, due to the numerical limitations discussed above, only the regime I with the large-amplitude deformation could be assessed numerically, while regime II and III have been studied in a qualitative manner. It is clearly desirable to extend the numerical studies also to these two regimes in the future.

6 Conclusions

By applying nonequilibrium thermodynamics in the form of the General Equation for the Non-Equilibrium Reversible-Irreversible Coupling (GENERIC), a concurrent two-scale model was developed to describe the nonlinear elasto-viscoplastic mechanical behavior of elastomers filled with hard nanoparticles. In particular, the major part of the work was devoted to incorporating the physical aging of the interparticle glassy material, which leads to the recovery of the elastic modulus with waiting time after large-amplitude oscillatory deformation. Doing so, the nanocomposite model developed in [5] is naturally extended by the thermodynamic modeling of physical aging and mechanical rejuvenation, that was studied for bulk glassy materials in [17,18]. The extension is based on the idea that the glassy interparticle amorphous system is considered as a sum of kinetic and configurational subsystems, and characterized by their specific entropies or equivalent temperatures, for which the evolution equations are formulated. Specifically, the evolution equation for the configurational temperature consists of two parts, representative of physical aging and mechanical rejuvenation, respectively.

The developed model has been studied numerically under oscillatory deformation. The specific deformation protocol followed in this study, described in Section 5.5, has been used in [8, 9] for studying the Mullins effect in a wider context. In this paper here, the same protocol is used to examine how the mechanical response of the entire nanocomposite is affected by physical aging and mechanical rejuvenation of the interparticle matrix material. Particularly, it is found that the model presented in this paper results in a recovery of the elastic modulus with waiting time. Although this is not yet giving a conclusive description of the Mullins effect, it is a valuable step towards a less phenomenological and more appropriate modeling of hard-particle filled elastomers.

With respect to the aging dynamics implemented in the above model, it must be pointed out that the evolution for the configurational temperature has its limitations. Considering a sample with $\theta > T$ (e.g. after a rapid quench to a low temperature), the contributions to the θ-evolution representative of physical aging and mechanical rejuvenation have opposite sign. By choosing the prefactor in the expression of τ_{R}, one can actually tune the limit to which θ can possibly increase due to mechanical rejuvenation, under certain loading conditions. In this sense, there is a coupling between this prefactor to τ_{R} and the loading condition, which seems unphysical. It is left as a task for future research to address this issue.

It was discussed that the numerical solution of the mutually coupled two-scale model is cumbersome. Specifically, the effect of mechanical rejuvenation on the configurational temperature of the matrix material contribution depends in an intricate way on the filler-particle arrangement. This dependence is of a type that makes it impossible, in general, to use the CONNFFESSIT approach for the numerical solution. In order to estimate the significance of the problematic contribution in comparison to other contributions, a Gaussian approximation was used. It turned out that under strong deformation, the problematic term can actually be neglected, and the quality of this approximation has been assessed. However, the limits of this numerical approximation are evident; particularly at small deformations and at equilibrium it is inappropriate. Therefore, this poses a task for the community of computational physics for the near future. Solving this issue is not only relevant for the specific work presented in this paper. More importantly, it can be envisioned that, as part of the ever increasing research activity in the field of multiscale materials modeling, other models of a similar kind will be developed that await to be solved with adequate numerical tools.

Acknowledgment

The authors gratefully acknowledge stimulating discussions with Hans Christian Öttinger, Jay D. Schieber, and Didier Long. This research was funded by the European Union through the project COMPNANOCOMP under Grant Number 295355, and forms part of the research programme of the Dutch Polymer Institute (DPI), project EU-FP-001 COMPNANOCOMP.

References

[1] T.A. Vilgis, G. Heinrich, M. Klüppel, Reinforcement of Polymer Nano-Composites: Theory, Experiments, and Applications, Cambridge University Press, Cambridge, 2009.

[2] S. Kaufman, W.P. Slichter, D.D. Davis, Nuclear magnetic resonance study of rubber-carbon black interactions, J. Polym. Sci. A2 9 (5) (1971) 829–839.

[3] J. Berriot, H. Montès, F. Lequeux, D.R. Long, P. Sotta, Evidence for the shift of the glass transition near the particles in silica-filled elastomers, Macromolecules 35 (26) (2002) 9756–9762.

[4] J. Berriot, H. Montès, F. Lequeux, D.R. Long, P. Sotta, Gradient of glass transition temperature in filled elastomers, Eur. Phys. Lett. 64 (1) (2003) 50–56.

[5] M. Semkiv, D.R. Long, M. Hütter, Concurrent two-scale model for the viscoelastic behavior of elastomers filled with hard nanoparticles, Continuum Mech. Thermodyn. 28 (6) (2016) 1711–1739.

[6] M.C. Boyce, D.M. Parks, A.S. Argon, Large inelastic deformation of glassy polymers, part 1, rate dependent constitutive model, Mech. Mater. 7 (1) (1988) 15–33.

[7] H.E.H. Meijer, L.E. Govaert, Mechanical performance of polymer systems: the relation between structure and properties, Prog. Polym. Sci. 30 (8–9) (2005) 915–938.

[8] S. Merabia, P. Sotta, D.R. Long, A microscopic model for the reinforcement and the nonlinear behavior of filled elastomers and thermoplastic elastomers (Payne and Mullins effects), Macromolecules 41 (21) (2008) 8252–8266.

[9] S. Merabia, P. Sotta, D.R. Long, Unique plastic and recovery behavior of nanofilled elastomers and thermoplastic elastomers (Payne and Mullins effects), J. Polym. Sci. Pol. Phys. 48 (13) (2010) 1495–1508.

[10] A. Papon, S. Merabia, L. Guy, F. Lequeux, H. Montès, P. Sotta, D.R. Long, Unique nonlinear behavior of nano-filled elastomers: from the onset of strain softening to large amplitude shear deformations, Macromolecules 45 (6) (2012) 2891–2904.

[11] L. Mullins, Effect of stretching on the properties of rubber, J. Rubber Res. 16 (1948) 275–282.

[12] L. Mullins, Softening of rubber by deformation, Rubber Chem. Technol. 42 (1969) 339–362.

[13] J. Diani, B. Fayolle, P. Gilormini, A review on the Mullins effect, Eur. Polym. J. 45 (3) (2009) 601–612.

[14] L. Mullins, Permanent set in vulcanized rubber, India Rubber World 120 (1949) 63–66.

[15] K. Kamrin, E. Bouchbinder, Two-temperature continuum thermomechanics of deforming amorphous solids, J. Mech. Phys. Solids 73 (2014) 269–288.

[16] R. Xiao, T.D. Nguyen, An effective temperature theory for the nonequilibrium behavior of amorphous polymers, J. Mech. Phys. Solids 82 (2015) 62–81.

[17] M. Semkiv, M. Hütter, Modeling aging and mechanical rejuvenation of amorphous solids, J. Non-Equilib. Thermodyn. 41 (2) (2016) 790–88.

[18] M. Semkiv, P.D. Anderson, M. Hütter, Two-subsystem thermodynamics for the mechanics of aging amorphous solids, Continuum Mech. Thermodyn. (2016) submitted.

[19] H.C. Öttinger, Nonequilibrium thermodynamics for open systems, Phys. Rev. E 73 (3) (2006) 036126.

[20] H.C. Öttinger, Bracket formulation of nonequilibrium thermodynamics for systems interacting with the environment, J. Non-Newtonian Fluid Mech. 152 (1) (2008) 2–11.

[21] M. Grmela, H.C. Öttinger, Dynamics and thermodynamics of complex fluids, part 1, development of a general formalism, Phys. Rev. E 56 (6) (1997) 6620–6632.

[22] H.C. Öttinger, M. Grmela, Dynamics and thermodynamics of complex fluids, part 2, illustrations of a general formalism, Phys. Rev. E 56 (6) (1997) 6633–6655.

[23] H.C. Öttinger, Beyond Equilibrium Thermodynamics, Wiley, Hobroken, 2005.

[24] T.M. Nieuwenhuizen, Thermodynamic description of a dynamical glassy transition, J. Phys. A-Math. Gen. 31 (10) (1998) L201–L207.

[25] F. Sciortino, W. Kob, P. Tartaglia, Inherent structure entropy of supercooled liquids, Phys. Rev. Lett. 83 (16) (1999) 3214–3217.

[26] A.Q. Tool, Relaxation of stresses in annealing glass, J. Res. Natl. Bur. Stand.(US) 34 (2) (1945) 199–211.

[27] L.F. Cugliandolo, J. Kurchan, L. Peliti, Energy flow, partial equilibration, and effective temperatures in systems with slow dynamics, Phys. Rev. E 55 (4) (1997) 3898–3914.

[28] T.M. Nieuwenhuizen, Thermodynamics of the glassy state: effective temperature as an additional system parameter, Phys. Rev. Lett. 80 (25) (1998) 5580–5583.

[29] H.C. Öttinger, Nonequilibrium thermodynamics of glasses, Phys. Rev. E 74 (1) (2006) 011113.

[30] E. Bouchbinder, J.S. Langer, Nonequilibrium thermodynamics of driven amorphous materials, part 2, effective-temperature theory, Phys. Rev. E, 80 (3) (2009) 031132.

[31] A.N. Beris, B.J. Edwards, Thermodynamics of Flowing Systems, Oxford University Press, New York, 1994.

[32] B.J. Edwards, An analysis of single and double generator thermodynamic formalisms for the macroscopic description of complex fluids, J. Non-Equilib. Thermodyn. 23 (4) (1998) 301–333.

[33] S.R. de Groot, P. Mazur, Non-equilibrium Thermodynamics, North Holland, Amsterdam, 1962.

[34] J.W. Gibbs, On the Fundamental Formula of Statistical Mechanics, with Applications to Astronomy and Thermodynamics, Salem Press, 1885.

[35] L.C.E. Struik, On the rejuvenation of physically aged polymers by mechanical deformation, Polymer 38 (16) (1997) 4053–4057.

[36] J.M. Hutchinson, Physical aging of polymers, Prog. Polym. Sci. 20 (4) (1995) 703–760.

[37] H.J. Kreuzer, Nonequilibrium Thermodynamics and its Statistical Foundations, Clarendon Press, Oxford, 1981.

[38] D.J. Evans, G.P. Morriss, Statistical Mechanics of Nonequilibrium Liquids, Academic Press, London, 1990.

[39] J.H. Irving, J.G. Kirkwood, The statistical mechanical theory of transport processes, part 4, the equations of hydrodynamics, J. Chem. Phys. 18 (6) (1950) 817–829.

[40] R.B. Bird, C.F. Curtiss, R.C. Armstrong, O. Hassager, Dynamics of Polymeric Liquids, vol 2: Kinetic Theory, 2nd edition, Wiley, New York, 1987.

[41] H.C. Öttinger, Stochastic Processes in Polymeric Fluids, Springer, Berlin, 1996.

[42] G. Adam and J.H. Gibbs, On the temperature dependence of cooperative relaxation properties in glass-forming liquids, J. Chem. Phys. 43 (1) (1965) 139–146.

[43] I.M. Hodge, Effects of annealing and prior history on enthalpy relaxation in glassy polymers. 6. Adam-Gibbs formulation of nonlinearity, Macromolecules 20 (11) (1987) 2897–2908.

[44] T.D. Nguyen, H.J. Qi, F. Castro, K.N. Long, A thermoviscoelastic model for amorphous shape memory polymers: incorporating structural and stress relaxation, J. Mech. Phys. Solids 56 (9) (2008) 2792–2814.

[45] J.D. Ferry, Viscoelastic Properties of Polymers, John Wiley and Sons, New York, 1980.

[46] M. Laso, H.C. Öttinger, Calculation of viscoelastic flow using molecular models: the CONNFFESSIT approach, J. Non-Newtonian Fluid Mech. 47 (1993) 1–20.

[47] C.W. Macosko, Rheology: Principles, Measurements, and Applications, Wiley-VCH, New York, 1994.